Using the Phase Angle Oscillator Controller for Hopping Robots:

by

Philip Wesley New

A Thesis Presented in Partial Fulfillment
of the Requirements for the Degree
Masters of Science

Approved April 2015 by the
Graduate Supervisory Committee:

Thomas G. Sugar, Chair
Sangram Redkar
Panagiotis Artemiadis

ARIZONA STATE UNIVERSITY

May 2015

ABSTRACT

As the robotic industry becomes increasingly present in some of the more extreme environments such as the battle field, disaster sites or extraplanetary exploration, it will be necessary to provide locomotive niche strategies that are optimal to each terrain. The hopping gait has been well studied in robotics and proven to be a potential method to fit some of these niche areas. There have been some difficulties in producing terrain following controllers that maintain robust, steady state, which are disturbance resistant.

The following thesis will discuss a controller which has shown the ability to produce these desired properties. A phase angle oscillator controller is shown to work remarkably well, both in simulation and with a one degree of freedom robotic test stand.

Work was also done with an experimental quadruped with less successful results, but which did show potential for stability. Additional work is suggested for the quadruped.

I would like to dedicate this thesis to the four most important people in the world: to my wife and partner, Danelle, to our son, Cameron, and to my parents, Frank and Mary Lou.

ACKNOWLEDGEMENTS

This thesis would never have been written if not for the help of Sandia National Laboratories, the National Physical Science Consortium, and the Human-Machine Integration Laboratory. I would also like to personally thank the following individuals for providing me with a sounding board and at times helping me to work through some interesting problems: Dr. Thomas G. Sugar, Chase Wheeler, Juan De La Fuente, and Andrew Bates.

TABLE OF CONTENTS

LIST OF TABLES

LIST OF FIGURES

Chapter 1

INTRODUCTION

1.1 A REVIEW OF THE STATE OF ROBOTICS

To start the discussion the definition of a robotic system which will be used in this thesis is laid out at the onset. It is the belief of this author that a robotic system is one which can sense an external event, make some logical choice based on the event, and then respond to the stimulus. In this respect the role robotics play has become ubiquitous in modern life.

We often do not recognize the presence of robots or their effect on our quality of life. When we do take notice of these systems, they are often not thought of as robotic. Have you walked through an automatic door? The system detected your presence, decided that a signal should be sent to an actuator, and then the actuator responded to the signal by opening the door.

The cost of many consumable products has been greatly reduced through increased production and efficiencies in manufacturing processes, largely due to robotics. Without the reduction in costs, many of the products we use in our everyday lives would either be out of our budget or perhaps unmarketable and unfeasible, and non-producible.

There are a number of robotic systems in current automobiles. One of the most recognizable among these is the anti-lock braking system (ABS) which assists us by preventing a vehicle operator from locking the brakes and wheels reducing or eliminating the skid. Skidding is particularly dangerous because in addition to increased stop times, a loss of steering occurs. This is a case where robotics have saved many lives and prevented injury over the past few decades.

Society has begun to ask more of robotic systems in the last few years in ways that will likely become profound. Some of the new and most exciting areas where robots are tasked are in Search and Rescue (SAR) scenarios [1] and military operations to help soldiers with battle field awareness, logistics and physical augmentation [2].

Wheeled robotics can and have been utilized in some of these capacities. This type of locomotion has been well studied, experimented on and explored. The advancements in wheeled robotics have been quite impressive in recent years as evident from the Google Car. The driverless car may become the norm in the near future [3]. Their areas of operation, especially when dealing with SAR or military missions where wheeled vehicles may lose their usefulness, is where the pavement meets the brush.

A potentially more effective mode of locomotion for rough terrain can be found with legged robotics. It is easy to imagine a four legged robot that could walk over obstacles three times greater than its hip height. If the length separating the hips were the same length as the ground to the hip, and the robot was then able to stand on one set of legs, it would then simply need to grasp the terrain above or be able to jump a relatively short distance to get its legs on the higher ground. If the legs were telescoping the height of an obstruction could be even greater.

Many legged configurations are possible. Robots are not limited to two or four legs. Theoretically, any number of legs could be used; the configurations are limited only by the imagination [4-6]. The diversity of potential configurations will lead to the development of niche robots that demonstrate high performance in those specific environments.

In addition to obstacle clearance, legged systems have benefits inherent to their design. Each leg provides an independent and isolated foothold for increased traction

and stability in rough terrain. Another advantage is that suspension is inevitably provided to the body when compliance is incorporated into the leg [7].

Control systems are needed to appropriately add energy for locomotion in legged robots such as monopedal, bipedal, or quadrupedal robots. Robust and stable control of these types of robots will be needed in many situations where wheeled robots do not perform well [8-10].

Systems can add energy based on negative damping [11], patterns based on phase angles [12,13], and impedance control [14]. A method has been developed to add energy to assist motion based on a phase angle.

The system adds a bounded amount of energy to create an oscillatory type of motion.

The control method has been shown to work on linear and rotary mechanical systems.

Two powered hoppers have been built and demonstrated using this new control method.

This phase-based approach is very powerful because a forcing function can be developed that acts on a hybrid dynamic system. Even though the dynamics change when the leg is contacting the ground in the stance phase and in the air during the flight phase, the forcing function does not change. It should be noted that in the case of these hopper robots versus some other phase angle controlled systems, the forcing function is not continuously active, rather is activated based on a phase angle and the control objective, i.e. operation in a steady state limit cycle or damping to zero velocity.

1.2 CONTRIBUTIONS

The contribution I have made to the field of robotics is the design and prototype development of a one degree of freedom hopper. It was the first hopping robot to

demonstrate that the phase angle, oscillator controller converges to a limit cycle. The experimental data from hopping showed extraordinary similitude to modeling. The robot and controller also displayed the desirable properties of stable hopping, resistance to disturbance, and convergence to a steady state regardless of initial conditions. I was the lead author on a 2014 IDETC Conference paper [15] about the one degree of freedom robot and co-author on a paper published in the ASME Journal of Mechanisms and Robotics [16] which discussed how the controller can enable limit cycles in robotic systems. I have also begun work on a quadruped robot that also uses the phase angle, oscillator controller. This work has shown potential to develop a stable hopper in simulation while work remains in the experimental domain.

1.3 THESIS ORGANIZATION

In Chapter 2 background information is given that is relevant to this thesis. The chapter describes the beginning of walking robots and how they have recently been asked to venture into the domain of the unpaved path for diverse purposes. Some of the current state of the art models are mentioned along with the inspiration for configurations and locomotive methods. This chapter also discusses what some researchers see as the need for a paradigm shift in thinking about the model most often used for hopping robots.

In Chapter 3 a phase angle oscillator controller is discussed. A mathematical description is given using the mass, spring, damper model. The model shows how a limit cycle is created by using the sine of the angle ϕ, which itself has the intrinsic limitation of having values between -1 and 1.

Chapter 4 discusses the extraordinary results the phase angle oscillator controller had with both a simulated and experimental one degree of freedom robot. A variety of

initial conditions were used and disturbances were added which all ended in the same limit cycle determined by the controller.

In Chapter 5 the discussion centers on the use of the phase angle oscillator controller on a quadruped robot and 2-dimensional simulation with two legs. While the results were not as conclusive as were those in Chapter 4, the results in this chapter do show there is some promise for this type of controller on multi-legged robots.

Chapter 6, the last chapter, is a conclusion which discusses gait strategies as well as some next steps for further research.

Chapter 2

BACKGROUND

One of, if not the earliest legged walking machines was designed around 1850 by the Russian mathematician Pafnuty Chebyshev. Since that time designers, scientists, researchers and imaginers have been trying to replicate what nature seems to have done so well. Make machines walk. Over the next 100 years, a number of systems have developed into successful machines [17].

In the mid 1980's Marc Raibert showed that hopping is a useful gait method for robots with his 3-D prototype and eventually with the "Monopod" [7]. Raibert's designs were mass, spring, damper systems that used compressed air to act as a spring to produce the effect of both a suspension system and an energy storage device.

The first use of robots for urban search and rescue (USAR) was at ground zero, World's Trade Center, 9-11-2001 [10]. The robots and their teams showed up six hours after the attacks. The primary use was to search for victims and to find paths through the rubble that would be easier and quicker to excavate. They also were used to help perform structural inspections and for detection of hazardous materials. These robots were both wheeled and tracked vehicles. The performance of the robots was considered a success as it was the first undertaking of a mission of this type. There were, however, limitations to the vehicles caused by the method of locomotion; objects jammed between the robot's body and tread stopping the robot. Treads also became un-tracked producing the same result. A recommendation for future robotic systems was the development of alternative strategies to climb obstacles like rubble piles and other obstructions.

Rough terrain becomes particularly problematic for wheeled and tracked vehicles. As a matter of practicality, wheels have a limited range in size. The terrain or obstacle in front of a tracked robot typically becomes impassible at 50% of track height.

In the case of wheels obstructions become road blocks around 40% of wheel height [18]. One could easily imagine that an off road robot may encounter an obstacle along a trail, such as a rock or a snag, that is four feet in height. This would require a robot to have a wheel height of over eight feet to surmount the object.

There is no intention to determine the practical limitation of wheel height in this paper. The reader can determine for him or herself where that line is. Understanding, however, that some limit exists and a possible method to deal with this situation is the purpose of this paper.

Wheels are also known to have a problem in soft dirt or loose rubble where they lose traction and spin out or go off course. Additionally they have the tendency to have a significant impact on the ground they cover by disrupting the soil, leaving tracks and ruts behind.

Zhuang, Gao, et.al [19] also make the argument that legged robots can navigate terrain that wheeled or tracked vehicles have trouble with. They surveyed many of the best current commercially available heavy duty legged robots to assess the state of performance in this type of robots. The mission of the robots they discuss range from forestry to military to space exploration; these include the Plustech Walking Machine [20], Boston Dynamics Big Dog [21] and LS3 [22], and NASA's ATHELETE [23]. They conclude that these robots can be well suited for outdoor exploration and disaster relief but many problems still exist. There are adverse efficiencies typically from poor leg design. There is a strong need for compliance and in most cases it is produced virtually instead of by direct compliance. Virtual compliance is the use of force sensors in an end effector to allow a robot to move in the direction of an externally applied force [24, 25]. This gives the appearance of compliance or a soft touch.

There is also a need to reduce computational complexity in the control algorithm. This problem appears to be common between both heavy-duty legged robots and their smaller counterparts. Zhuang specifically suggest that further research should aim to develop a simpler intelligent control algorithm that meets compliance requirements.

Many of the current legged robots gaining attention draw from biologically inspired locomotion. Two biological mentors are humans for the gait of bipedal robots and the cheetah for quadrupeds [26]. One of the lessons being learned in studying biology is in the direct compliance mode animals and insects use. Direct compliance in animals comes from tendons and ligaments which act much like springs giving way to a force when pushed on. These natural springs are in series with the actuator, in this case muscle. The model generally used to describe the gait of an animal is a mass, spring, damper system.

A distinct advantage for the animal is that while walking or running, as the tendons and ligaments give position, they are storing energy that can be released in the next gait cycle or in the next part of the current gait cycle. The ability to store energy from within the gait cycle improves efficiency, while allowing for faster speeds, and greater leaping ability. Because robots, particularly hopping robots have a flight phase, this means that obstructions can be avoided by jumping higher.

Tendons or springs act as shock absorbers reducing impact forces and improving path following while walking or running. Animals have also been shown to change the angle of limbs during impact which effectively changes the limb compliance. This allows for better and more reactive control when experiencing sudden changes in speed, payload or terrain. Typically the method of integrating direct compliance into a leg design is made by using steel coil springs, compressed air or compliant mechanisms. All

three have been proven to be used effectively and are chosen based on a robot's primary objective.

While looking toward biology to inspire the next evolution in robotics has proven to be valuable, it should be noted that the systems we see in nature have been evolving due to natural selection over many millions of years. Research is only beginning to gain a modest understanding of the interplay of these natural systems on a high degree of freedom musculoskeletal structure. Additionally a number of animal components serve multiple purposes which speak to the efficiency of these bodies.

The human walking gait can be modeled as a ballistic motion where the center of mass reaches an apex and begins to fall toward the ground, allowing gravity to do the work for us [27]. Similarly, work has been done to show that ballistic modeling of walking in quadrupeds is valid [28]. This study concentrated on a bounding gait, an amble, and a trot. Although the three gaits were all ballistic, there were no flight phases among them.

From ballistic models, it is an easy step to assume that the gait becomes analogous to hopping. Bounding quadrupeds are generally thought to be using a type of hopping gate. If you watch the center of gravity of a running biped, the motion is akin to hopping as well.

In a study published in 2010 hopping in humans and robots were studied [29]. They suggest that current research has used apex-preserving hopping as the model for human and robotic hopping. In their opinion this model should be replaced with a spring, mass, damper system that utilizes a constant energy supply. A constant energy supply means that every cycle of the gait receives the same energetic input no matter what are the states of the hopper. As a system experiences dissipative losses of energy

from damping and friction, the energy injection, in theory, will compensate for the losses.

The paradigm of the hopping model as apex-preserving to one of terrain following will result in a more robust, disturbance resistant hopper and one which is less computationally demanding. They suggest that the energy dissipation itself is an essential component to stable, steady state hopping instead of being an intrinsic perturbation to the system.

A question that comes out of the paper is "does there exist a solution that guarantees energy losses high enough to produce robust and stable terrain following hopping?" The authors propose that the Hill-type muscle model may produce the desired result.

This model utilizes a force-length and force-velocity relationship to produce stability and a damping of effects from perturbations. It also uses a contractive element along with both a series and parallel elastic element [30, 31]. A mechanism, if it existed, also could use these relationships and elements to produce a system with the same stability as the model.

Many similarities exist between the Hill-type muscle model and the one degree of freedom hopper and the phase oscillator control system discussed in this thesis. The model and the robot both have contractive elements, with a series and parallel elastic element. The foot of the 1 degree of freedom hopper is a spring. The spring acts in series with the robot and in parallel to the actuator. The control system of the robot has similarities to the force-length and force velocity relationships used in the model. A phase diagram is created for the robot's control which plots the position of the spring against the velocity of the spring. The phase oscillator control is not an exact correlation

to the Hill-type model's force-length and force velocity control since force is not considered as part of the control.

The most important similarity, however, is the result of a stable controller that is resistant to disturbances and converges on a steady state independent of initial conditions.

Chapter 3

CONTROL SYSTEM DESIGN

Phase plane analysis can be studied to determine if the system moves in a repeating cycle or limit cycle [32]. In this work, a non-linear forcing function is used based on the sine of the phase angle. Because the sine function can never be greater or smaller than one or negative one, the function is bounded.

A standard, second order, mechanical system equation is given: m represents the mass, b represents the damping, k represents the stiffness.

$$m\ddot{x} + b\dot{x} + kx = 0 \tag{1}$$

Groups have added negative damping to systems to force a system to move, but the negative damping can become unstable because $c\dot{x}$ grows as the velocity gets larger.

$$m\ddot{x} + b\dot{x} + kx = c\dot{x}, where\ c < 0 \tag{2}$$

The control system described here adds energy to the mechanical system by using a "phase oscillator". It uses the sine of the phase angle, $\emptyset$. In Figure 3.1, the phase angle, $\emptyset$, is defined.

$$m\ddot{x} + b\dot{x} + kx = c\sin(\emptyset) = \frac{c\dot{x}}{\sqrt{\dot{x}^2 + x^2}} \tag{3}$$

If c is positive, the system oscillates back and forth. The energy is always bounded because as $\dot{x}$ becomes larger than x in the limit, the numerator and denominator cancel and just equal c, see Figures 4.17 and 4.18 in Chapter 4.

If c is negative, the energy is damped, and the system state goes to zero, see Figures 4.11 and 4.12 in Chapter 4.

In a simulated example, an external force is applied to a one degree of freedom hopper based on the sine of the phase angle. The external force causes the system to

oscillate up and down. In order to represent the physical system an external force is set to act on the system only while the phase angle is between 91˚ and 90˚, see Figure 3.2,

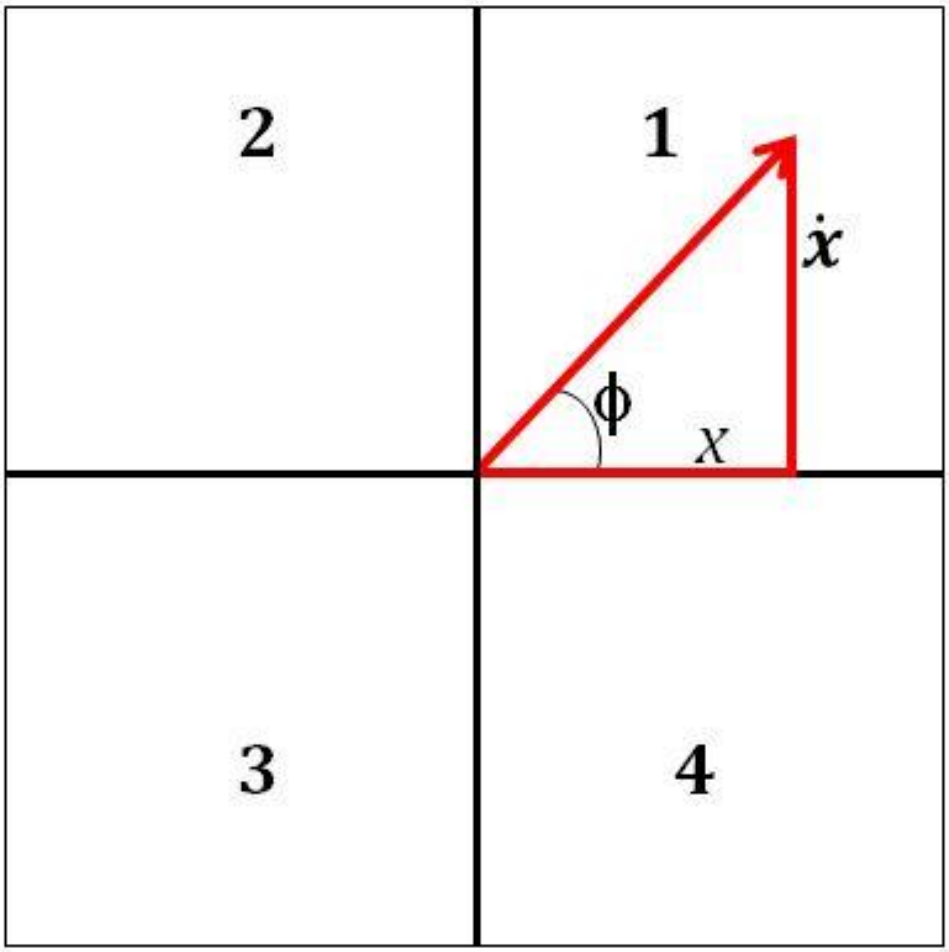

Figure 3.1: Phase plot definition, horizontal axis is the position, x, and the vertical axis is the velocity, $\dot{x}$. The sine of the phase angle phi is given by the opposite over the hypotenuse. The hypotenuse is given by $\sqrt{\dot{x}^2 + x^2}$.

which represents the moment just prior to the hopper becoming airborne. This allows the spring to transfer all of its energy back into the system augmenting the external force. The hopper has a mass of 0.6 kg and the spring stiffness and damping parameters equal 2469.3 N/m and 1.1 N/(m/s) respectively. The spring stiffness is only active once the hopper hits the ground and remains active until it returns to the air. An external gravity field is present and reduces the upward velocity.

$$m\ddot{x} + b\dot{x} + (kx * e(x)) + mg = c\sin(\emptyset) = \frac{c\dot{x}}{\sqrt{\dot{x}^2 + x^2}} \tag{4}$$

$$e(x) = \begin{cases} 1, & if\ x < 0 \\ 0, & if\ x \geq 0 \end{cases} \tag{5}$$

In the simulated example, see Figure 3.2, c = 33 N, m = 0.6 kg, b = 1.1 N/(m/s), k = 2469.3 N/m.

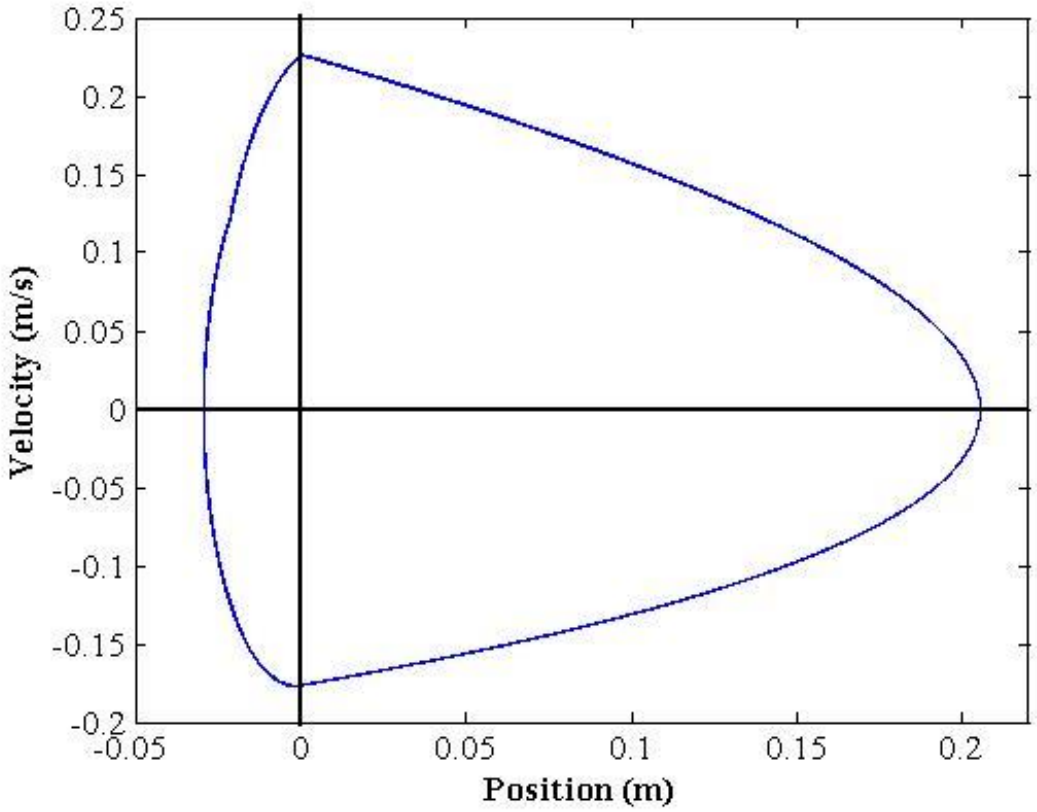

Figure 3.2: Simulated phase portrait of robotic hopper.

The limit cycle is robust and a wide range of initial conditions converge to the hopping cycle defined by the constant *c*. The system oscillates up and down; Figures 4.8 and 4.14 in Chapter 4 are examples of varied initial conditions.

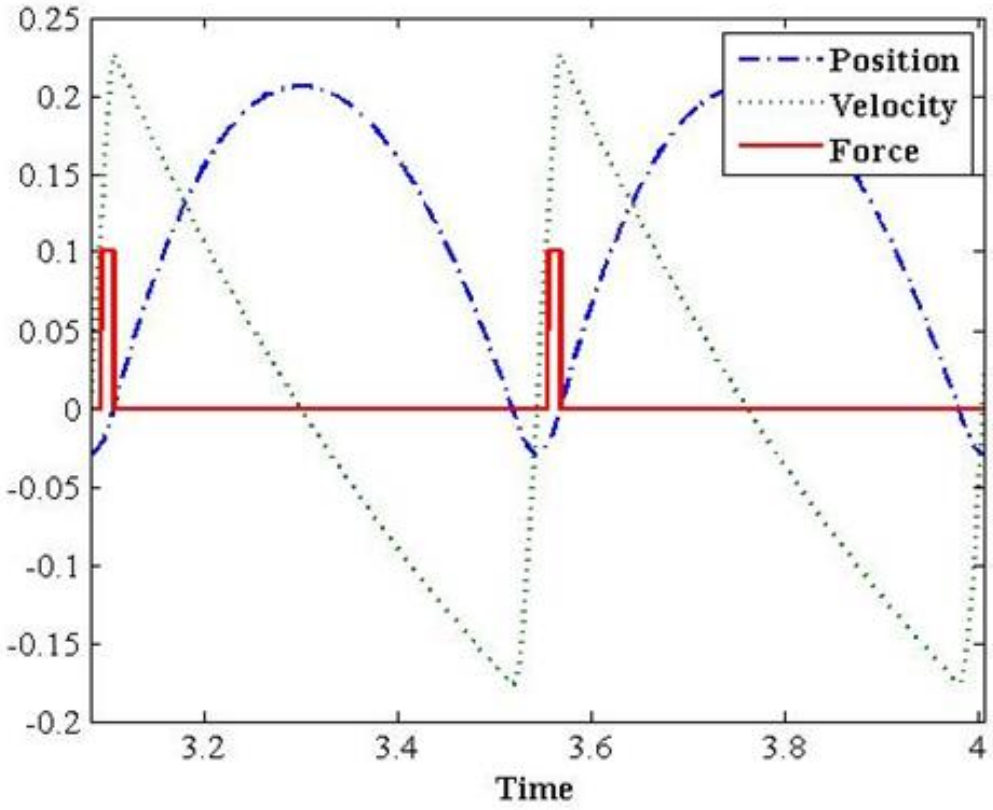

Figure 3.3: Simulated position, velocity and forcing function.

Chapter 4

ONE DEGREE OF FREEDOM HOPPER

4.1 DESCRIPTION OF A ONE DEGREE OF FREEDOM ROBOTIC HOPPER

The one degree of freedom hopper consists of an actuator and spring in series with the body and in parallel to the actuator. This is clamped to a ball bearing carriage and

Figure 4.4: One Degree of Freedom Robotic Hopper Assembly.

attached to a vertically mounted linear rail, Figure 4.4. This configuration allows free vertical motion.

The actuator is a ¾ inch, dual actuated, pneumatic cylinder. The cylinder has been glued into off-the-shelf PVC parts. Holes were drilled through the PVC to allow access to the input and output ports of the actuator. A spring has been glued to the lower end of the PVC fittings. The actuator rod deploys through the center of the spring. A digital encoder is attached to the carriage so that it can read a linear transmissive strip that has been attached to the rail mount. The rail is mounted to a 21"x 1-¾ "x ¾" aluminum bar. The bar is attached to a base plate (4"x 7"x ¾ ") of the same stock.

A 24V bidirectional valve connects regulated lp (low pressure) air to the actuator. The valve's switch is controlled by a Digilent Cerebot MC7 board. Matlab code is generated using Simulink Coder and the code is transferred to the microprocessor board.

Figure 4.5 shows the component block diagram for easy visualization of the robot system.

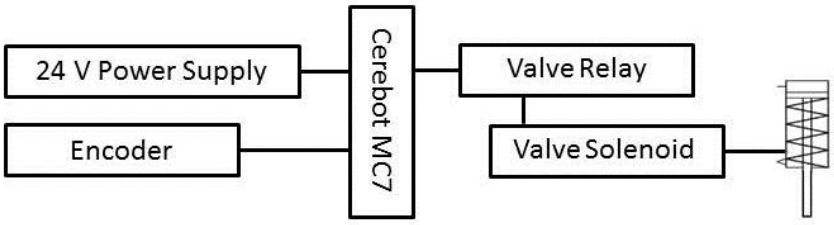

Figure 4.5: Block diagram showing component configuration of the system.

4.2 SIMULATED VS. ACTUAL RESULTS

The following figures show the Simulink simulated results compared to actual data collected. The physical parameters of the simulation are the same as mentioned previously in Chapter 3. The mass of the hopper is 0.6 kg, spring rate is 2469.3 N/m, damping factor is 1.1 N/m/s and the external force, if applied, is 33 N.

In the first experiment the model was simulated with the initial position at 0.2465 m and no external force was applied. The robot was also tested by dropping from the same initial height. The system controller was off in order to verify that the simulation parameters and physical system matched.

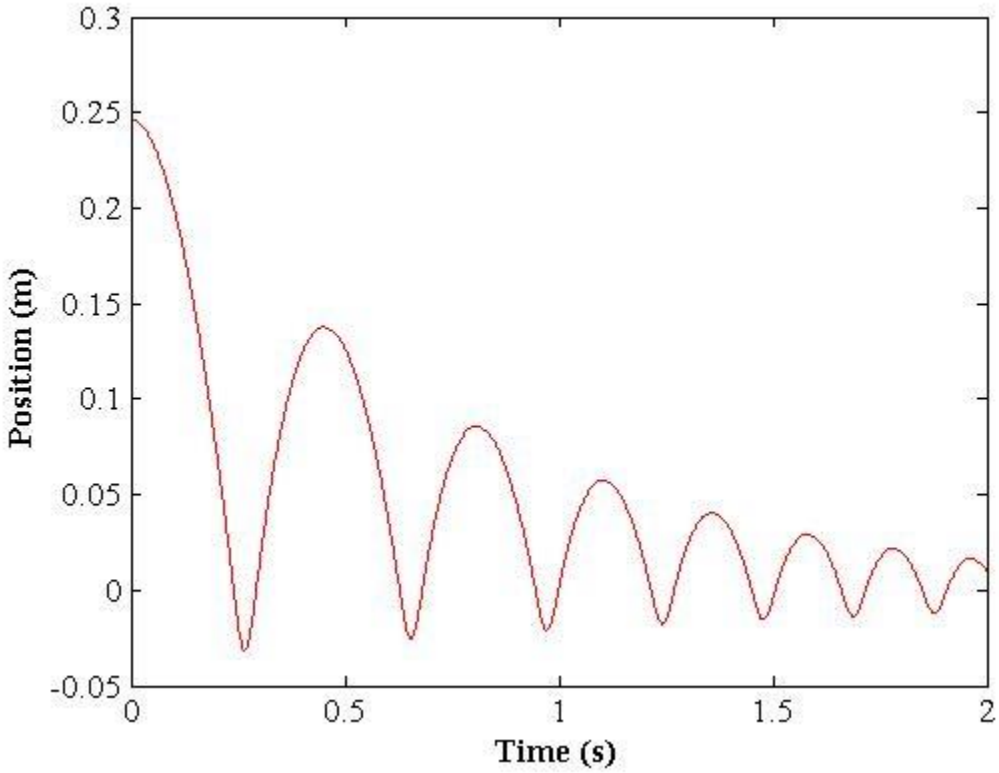

Figure 4.6: Simulated position vs time of hopper dropped from an initial height of 0.2465m.

Figures 4.6-4.8 show that the simulation is comparable to the physical system and any variations are due to nonlinearities in the latter.

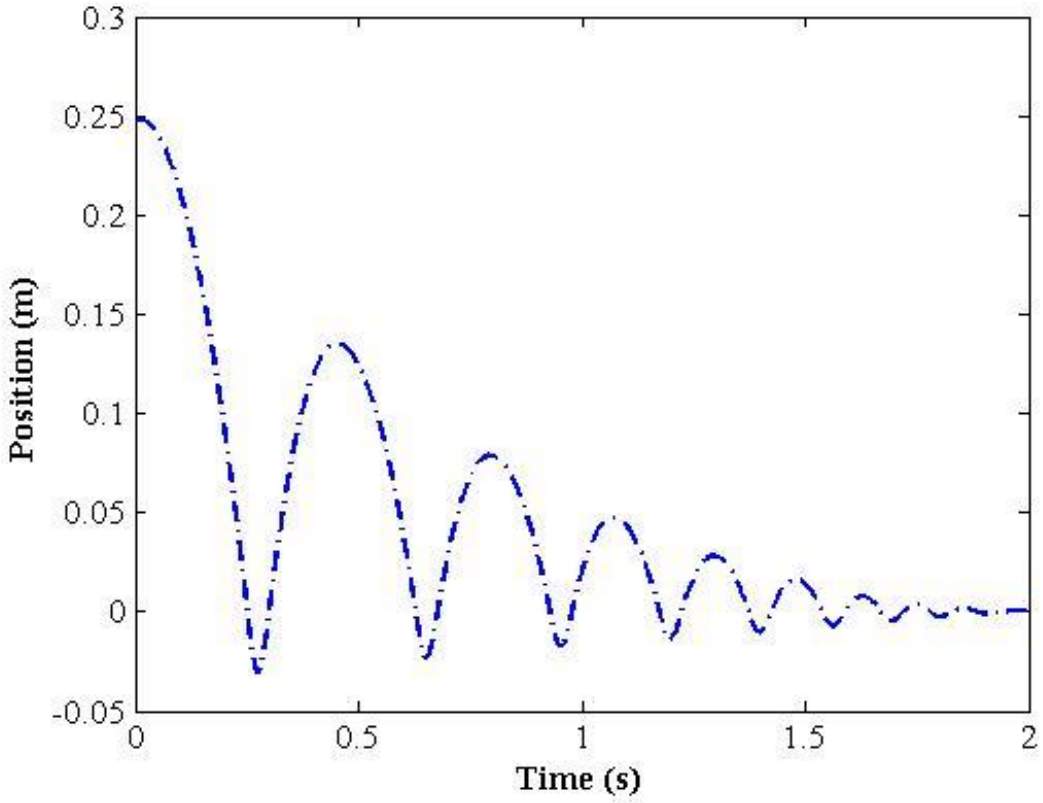

Figure 4.7: Actual position vs time of hopper dropped from an initial height of 0.2465m.

The following trial simulated and tested the hopper as it was dropped from an initial height of 0.2465 m with the controller on allowing the addition of energy just as the hopper is leaving the ground. Figures 4.9-4.11 show that after only a few hops, both the simulated and physical hopper reach steady state.

If the controller is activating the hopper's rod out of phase with the hopper the hopping is damped to zero. This was simulated this by making c = -33 N and by reversing the control command in the physical system so the actuator would fire out of phase with robot. Figures 4.12-4.14 show the results of implementing the controller out of phase. Notice this method caused the cylinder to fire before the hopper hit the ground resulting in smaller hops that ultimately damped the system to zero.

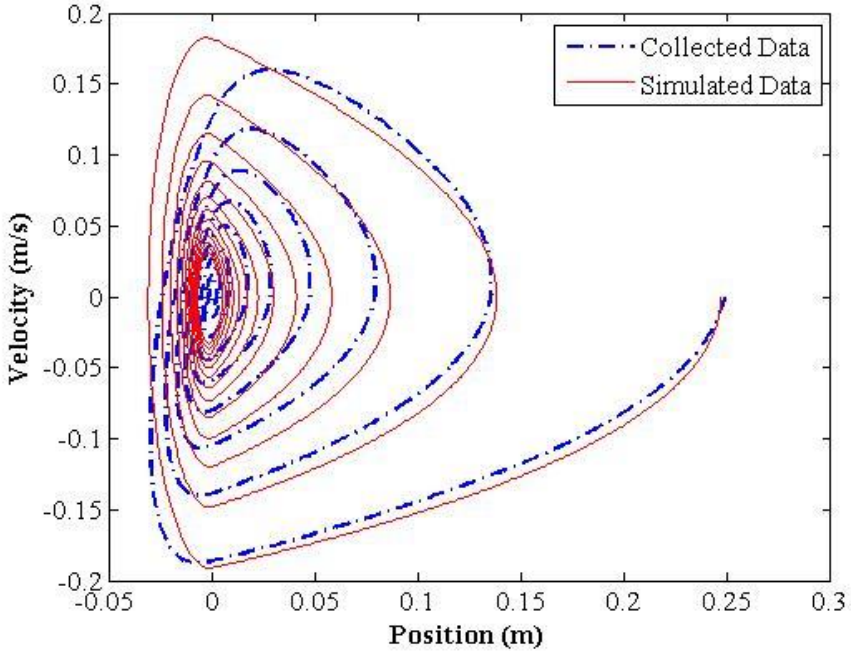

Figure 4.8: Phase portrait of hopper dropped from an initial height of 0.2465 m with the controller off.

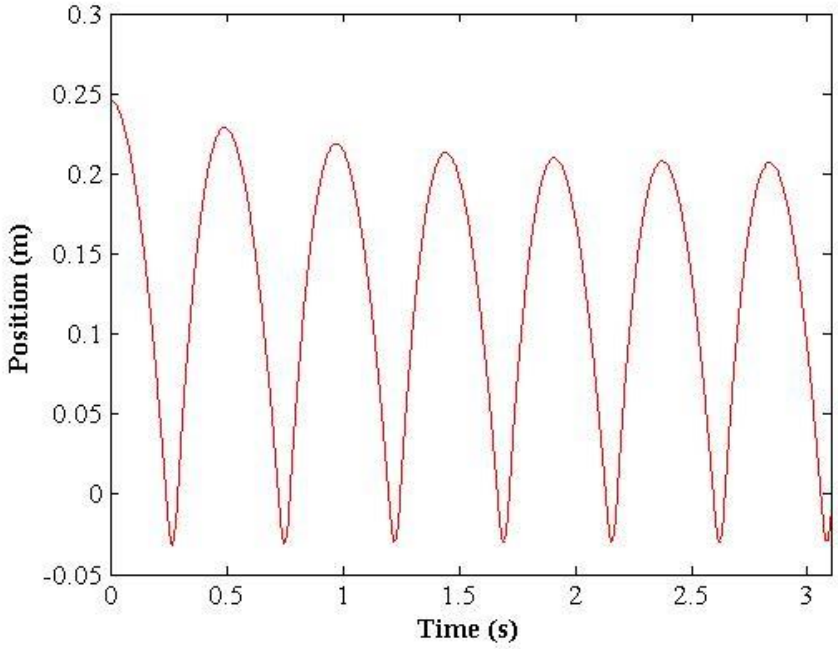

Figure 4.9: Simulated position vs time of hopper dropped from an initial height of 0.2465 m with the controller on.

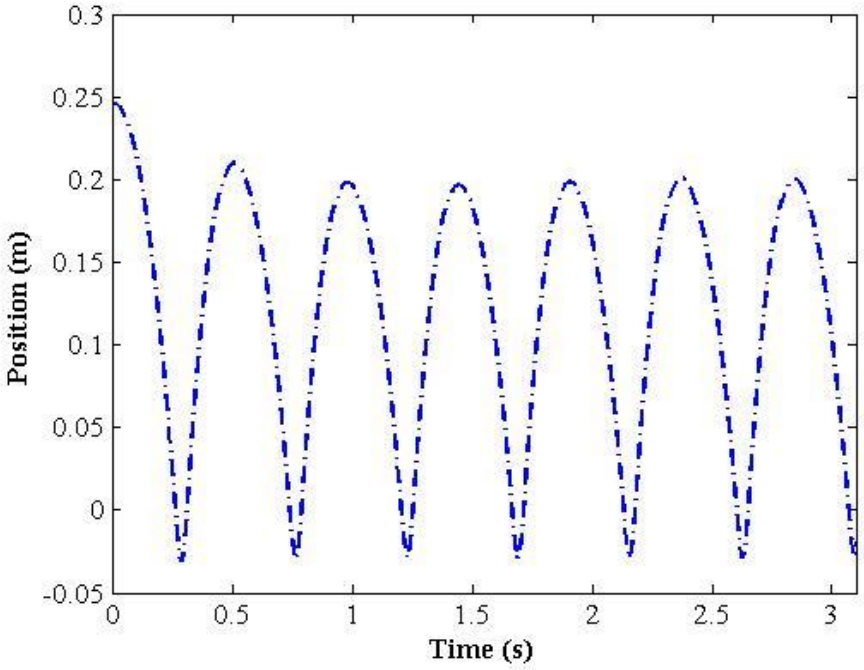

Figure 4.10: Experimental position vs time of hopper dropped from an initial height of 0.2465 m with the controller on.

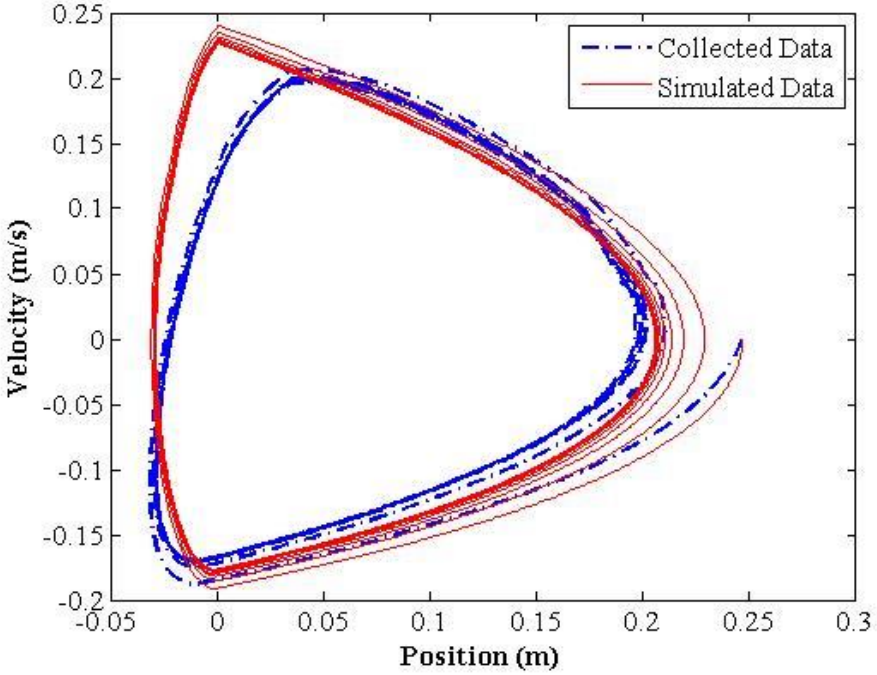

Figure 4.11: Phase portrait of hopper dropped from an initial height of 0.2465 m with the controller on.

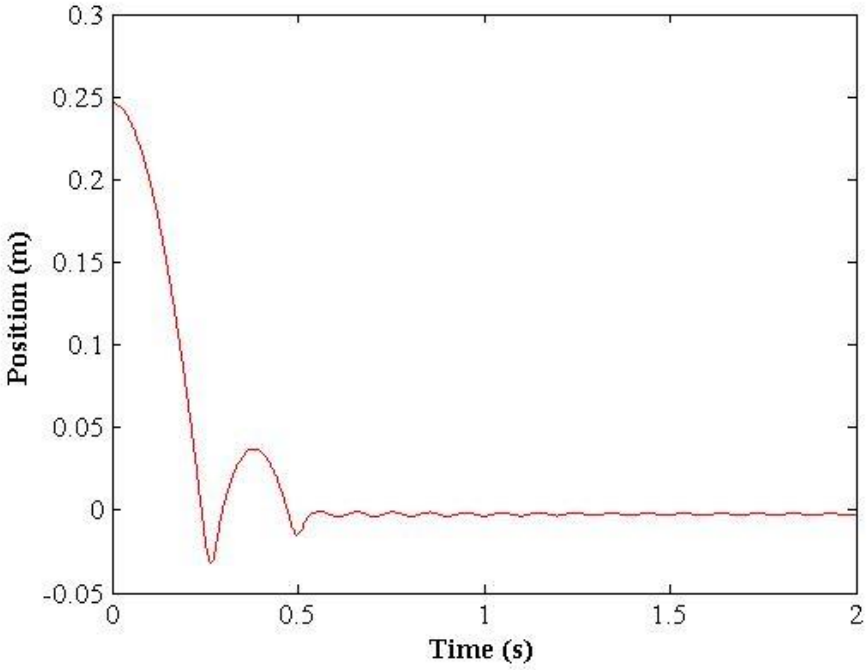

Figure 4.12: Simulated position vs time of hopper dropped from an initial height of 0.2465m with the controller reversed.

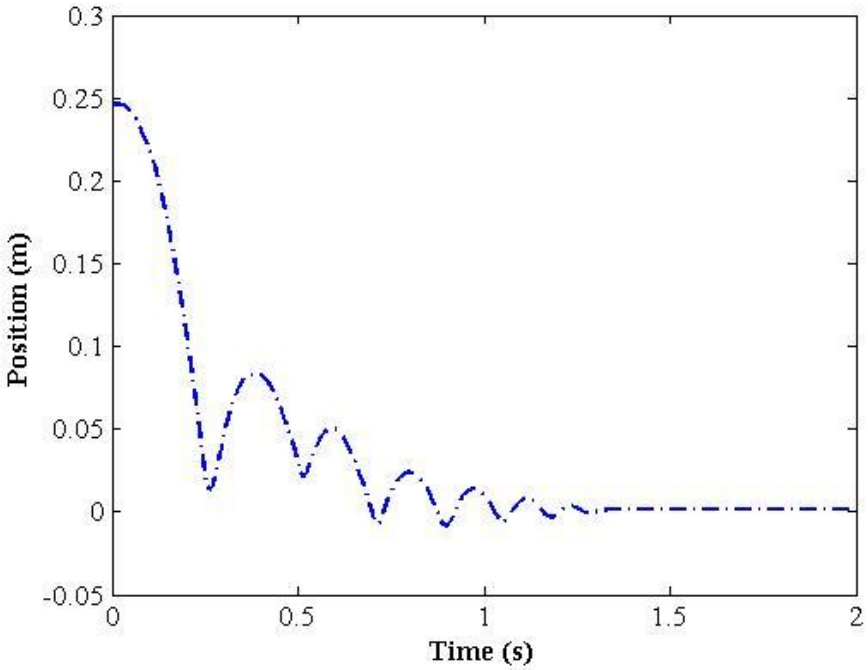

Figure 4.13: Experimental position vs time of hopper dropped from an initial height of 0.2465m with the controller reversed.

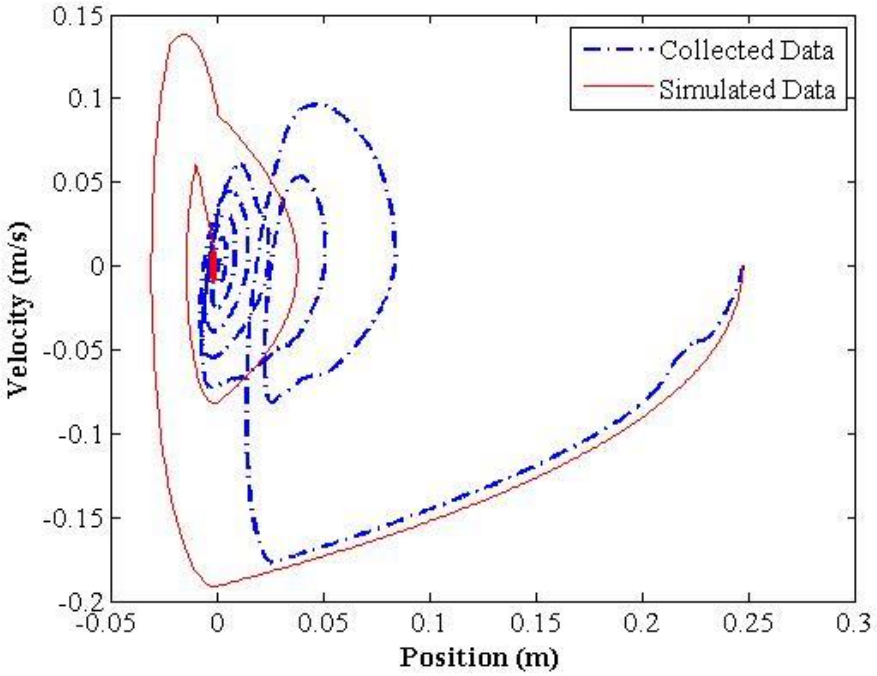

Figure 4.14: Phase portrait of hopper dropped from an initial height of 0.2465 m with the controller reversed.

Figures 4.15-4.17 show the simulated and experimental transient response from rest to steady state. To begin the data collection a pushbutton manually actuated the cylinder. The graphs show that both the simulation and physical system take about 2.5 seconds to reach steady state.

Figures 4.18-4.20 show the system at steady state.

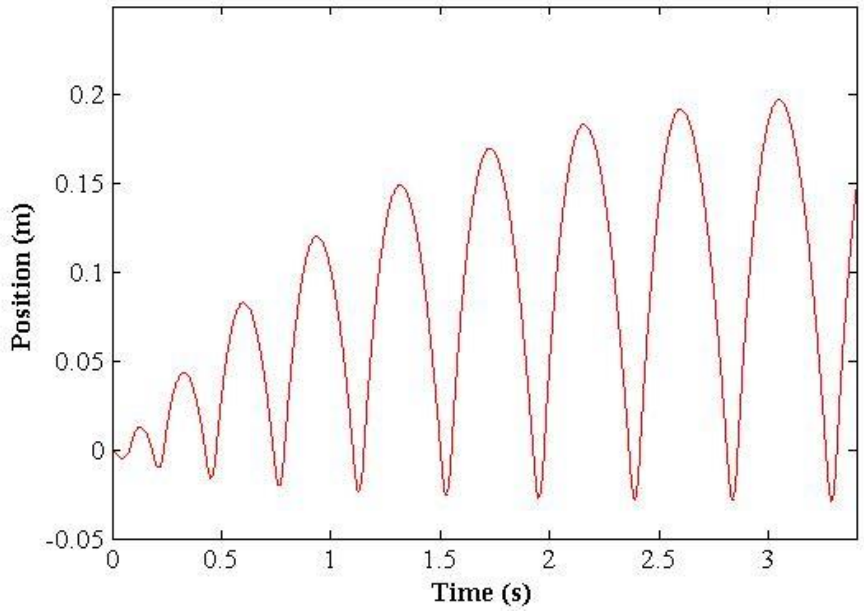

Figure 4.15: Simulated position vs time of the hopper in its transient state from an initial position of zero to steady state.

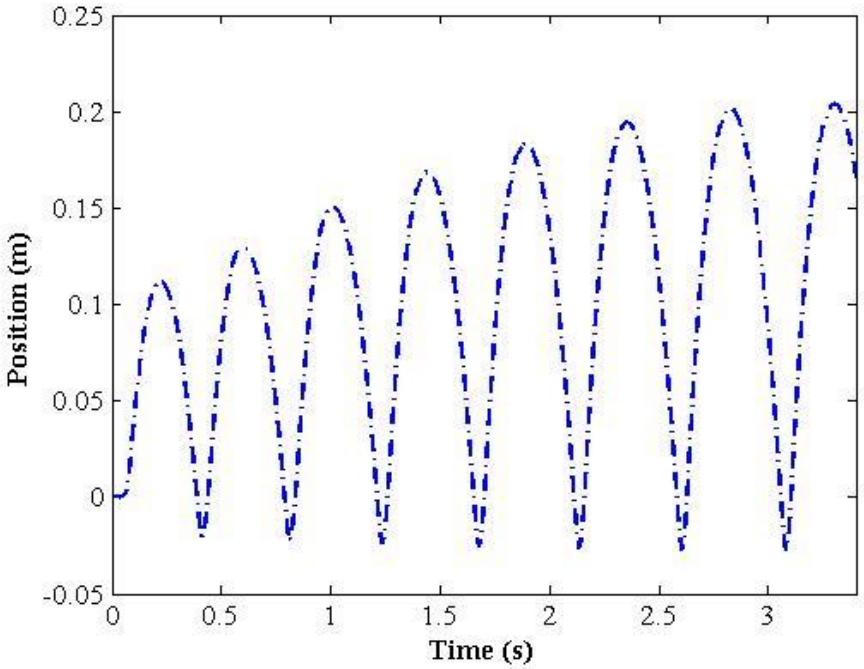

Figure 4.16: Actual position vs time of the hopper's transient response from an initial position of zero to steady state.

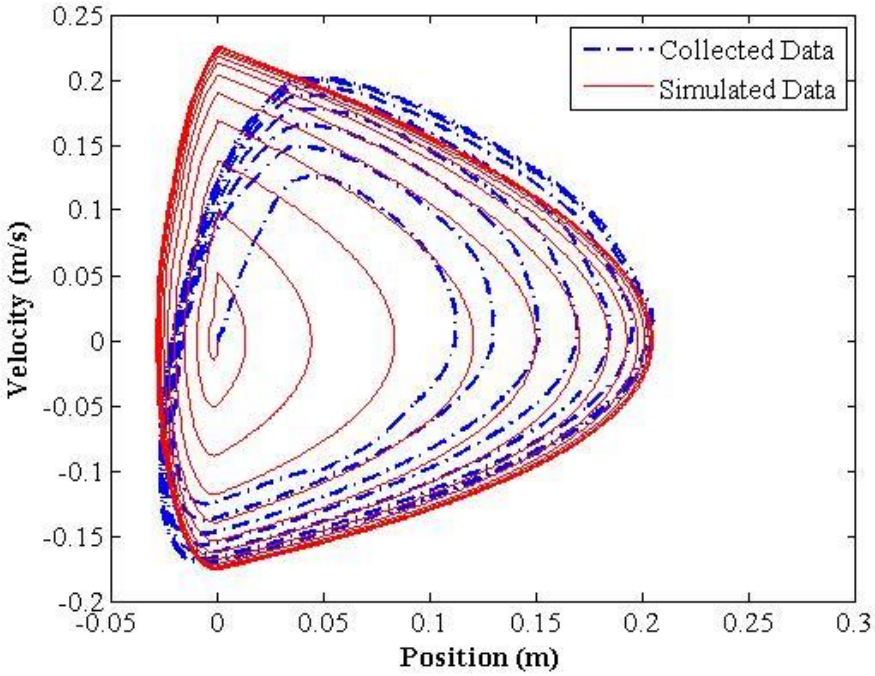

Figure 4.17: The transient phase portrait of the hopper from rest to steady state.

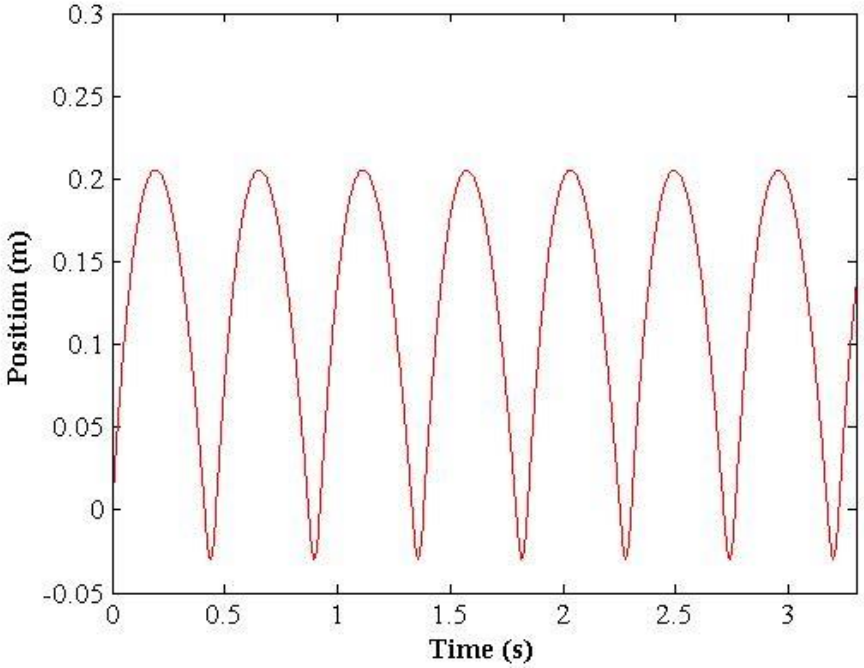

Figure 4.18: Simulated position vs time of steady state.

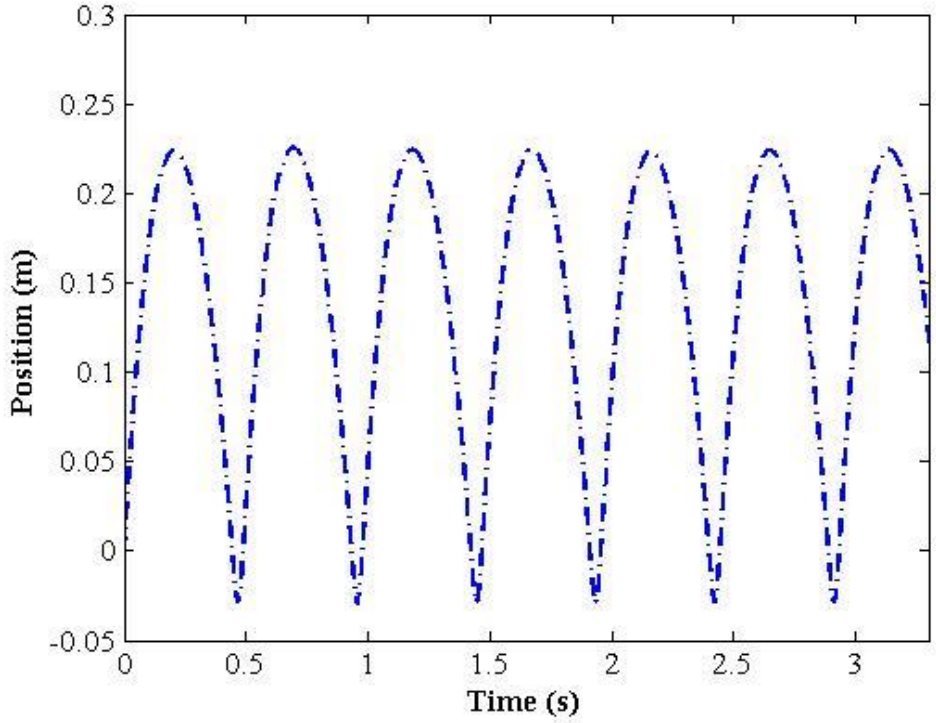

Figure 4.19: Actual position vs time of steady state.

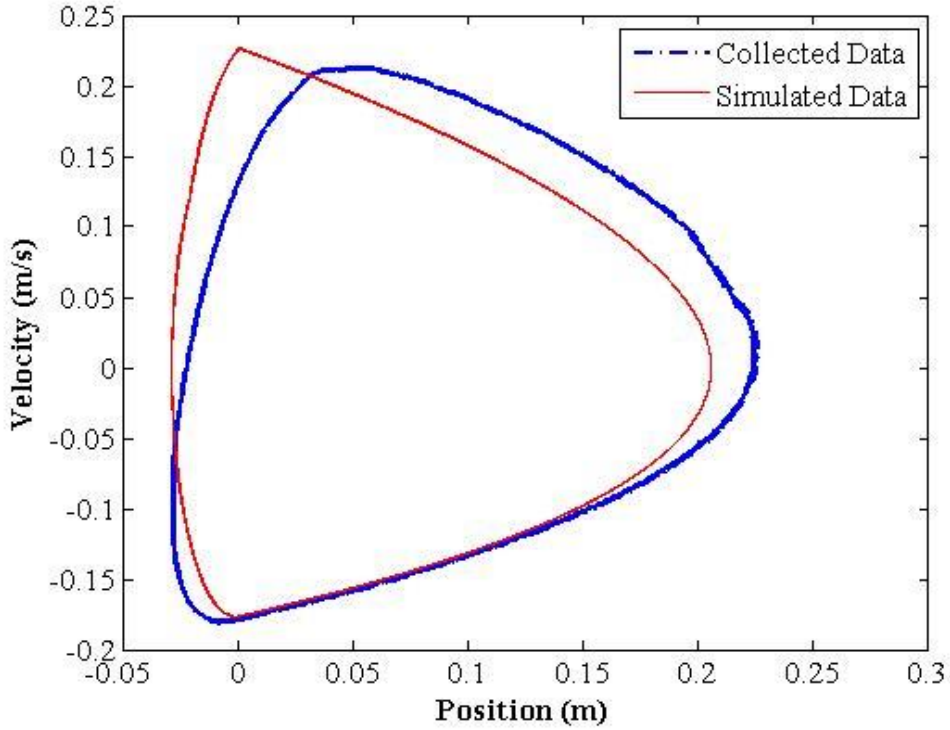

Figure 4.20: Phase portrait of hopper at steady state.

The controller is very robust to disturbances. One can bang on the top of the system or hold a wooden block against the system to limit hop height. In one example, Figure 4.21 and 4.22, a hand blocks and disturbs the hop height. The system is disturbed, and returns back to a stable limit cycle. In a second example, a wooden block was used to limit the hop height. In this example, the system moved to a new stable limit cycle with a reduced hop height, but an increased hopping frequency.

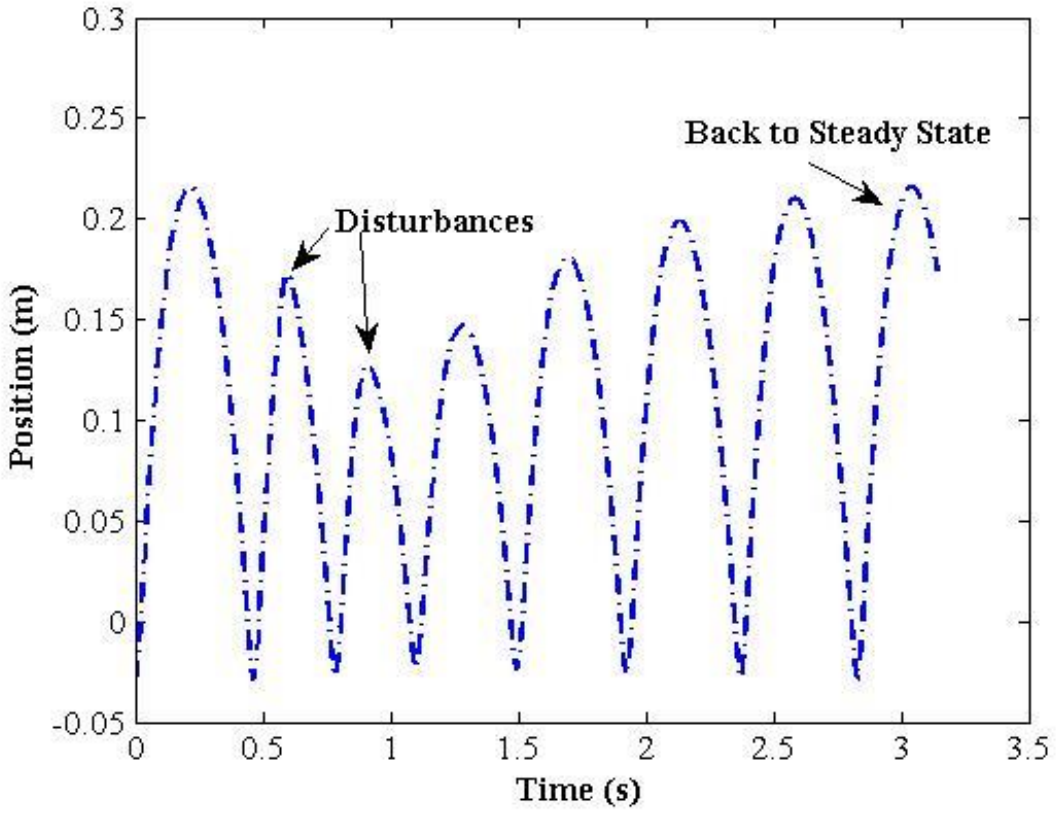

Figure 4.21: Actual position vs time of hopper experiencing two disturbances which limited height.

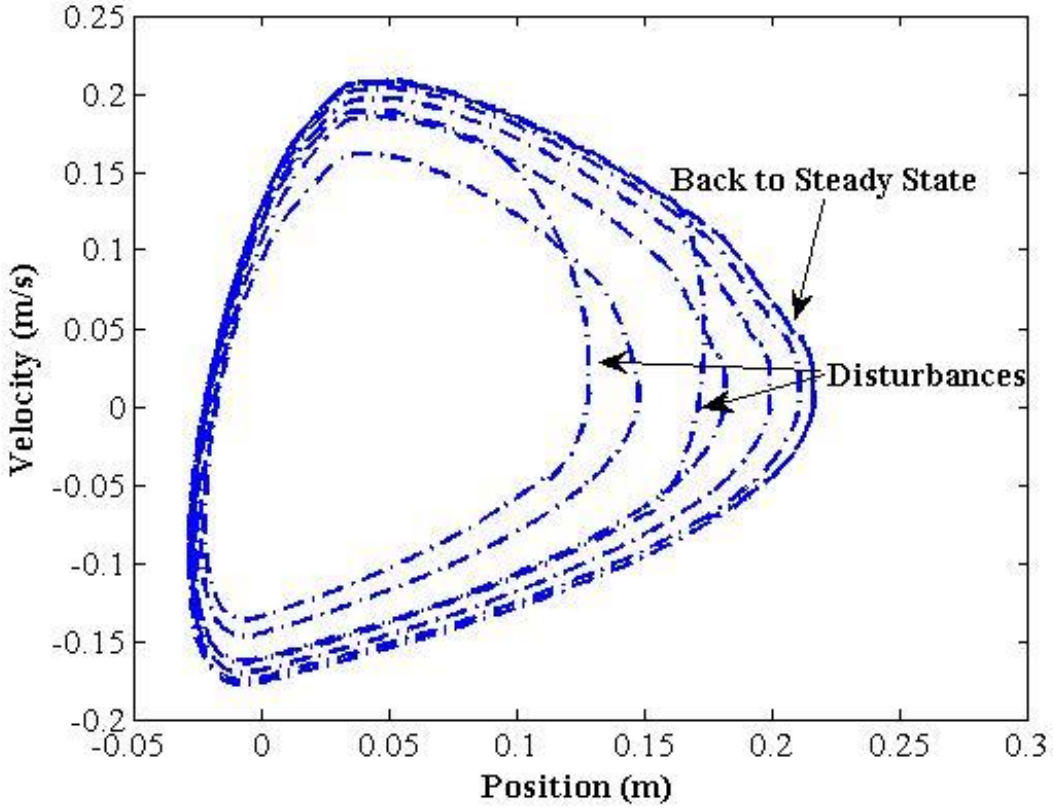

Figure 4.22: Phase portrait of hopper experiencing two disturbances which limited height.

Chapter 5

QUADRUPED HOPPER

5.1 DESCRIPTION OF QUADURPED HOPPER

The quadruped leg design was built on the strategy of the 1DOF hopper. A version of the 1DOF hopper was used for each individual leg. A pneumatic cylinder is the actuator and a spring 1.23k N/m is used for direct compliance and to return energy to the system as it hopped.

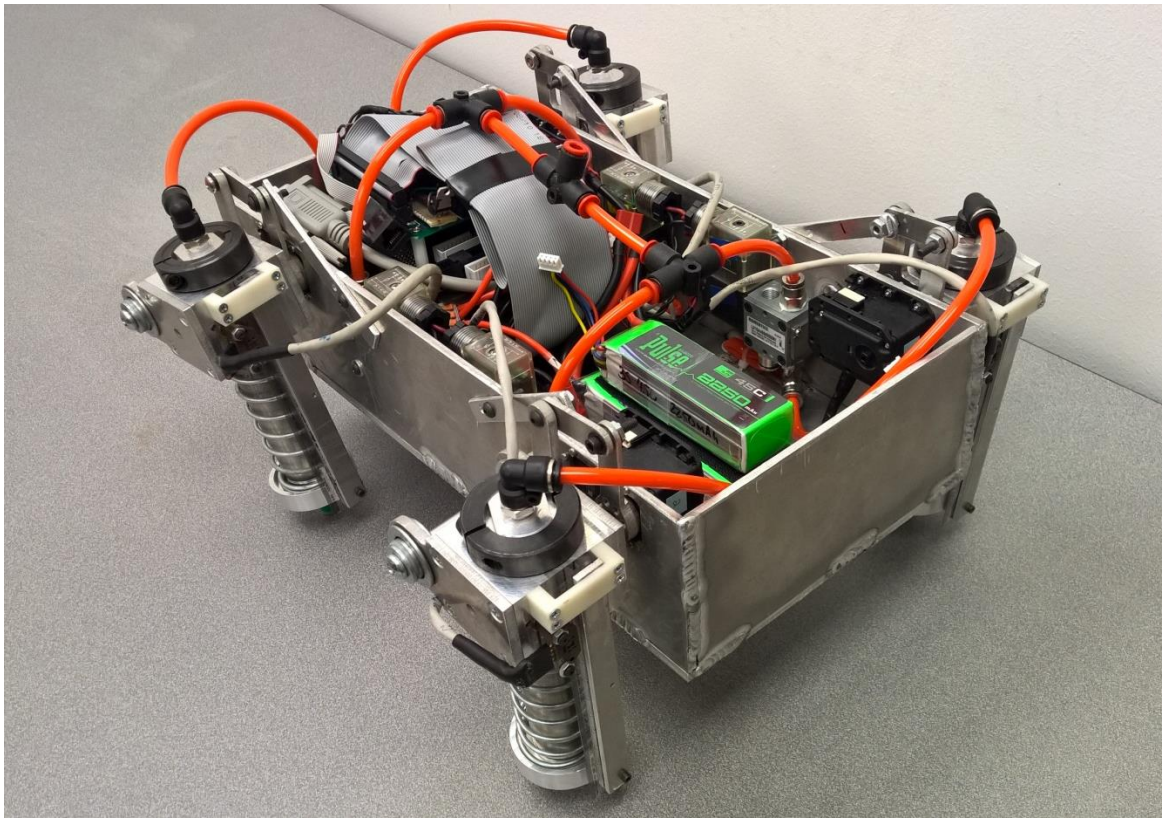

Figure 5.23: Experimental 4DOF hopping robot.

Although similarities exist between the hoppers, there are some major modifications to the quadruped leg. As a result of having four legs in a rectangular configuration (Figure 5.23), the robot is statically stable therefore the robot can stand

alone and the slide bearing and rail used in the one DOF hopper are longer necessary to maintain the proper attitude. The leg is attached to the body through a rotary joint and a four bar linkage system with the motors. The spring on the 4DOF leg has been moved over, or around, (see Figure 5.24) the body of the cylinder as opposed to acting as the foot in the 1DOF version. This was done to reduce buckling in the spring since the robot was no longer assured of purely vertical motion.

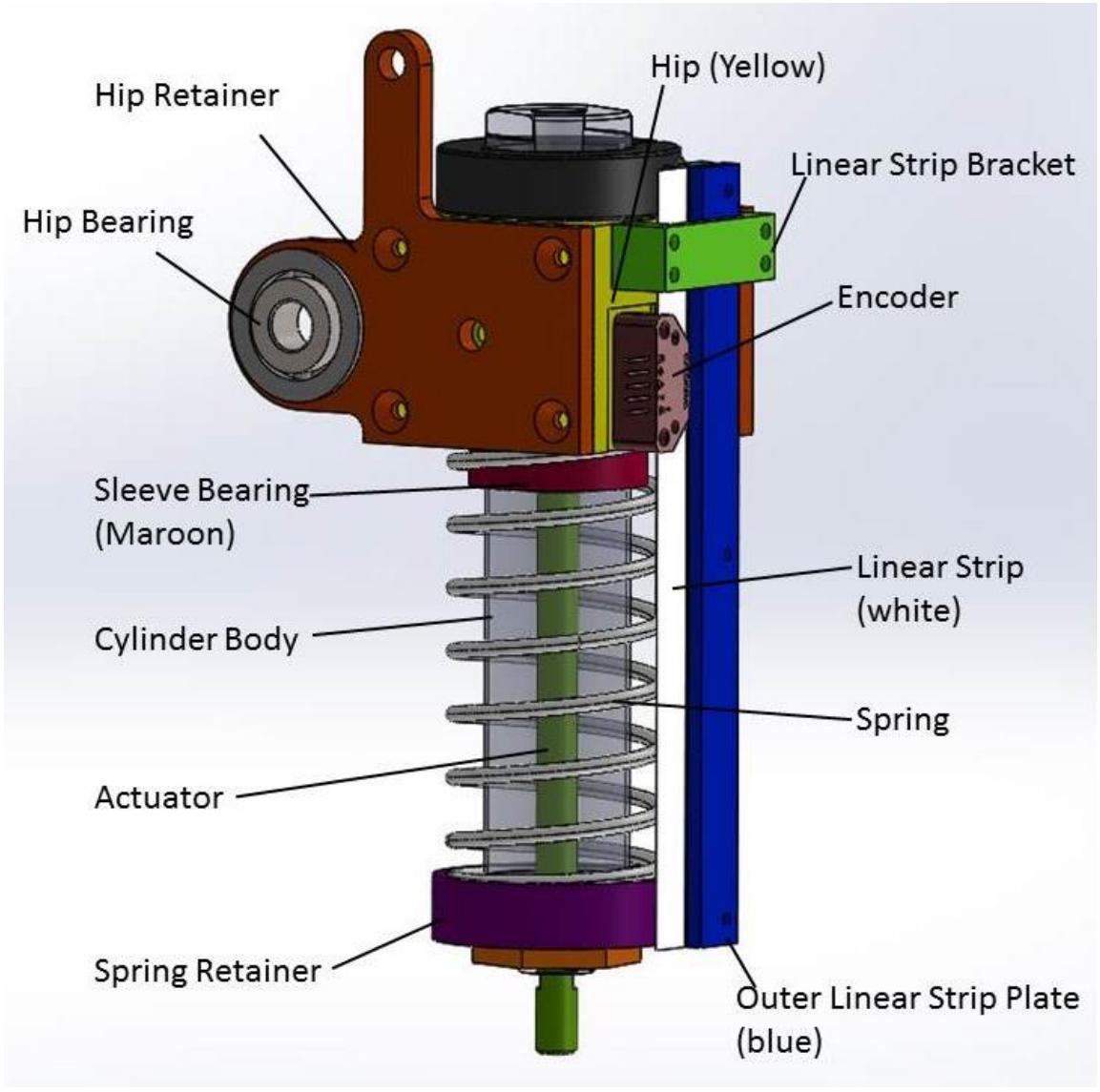

Figure 5.24: CAD drawing of one leg of the 4 DOF hopping robot.

The method of mounting the US Digital EM1 Transmissive Optical Encoder and linear strip was reconsidered since the bearing rail was the mounting surface on the 1DOF robot. The linear strip (colored white in Figure 5.24) was secured between two plates. It was decided that the one end of the plates could be attached to the spring retainer. The spring retainer was secured in place on the foot end of the cylinder. The linear strip plates (Dark blue and light blue in Figure 5.24) were held in place by a bracket as well as the spring retainer. A notch was added to the hip and a grove was cut into the inner linear strip plate. The notch slides in the groove to ensure that the linear strip is always in the proper place to be read by the encoder. This feature is not shown in Figure 5.24.

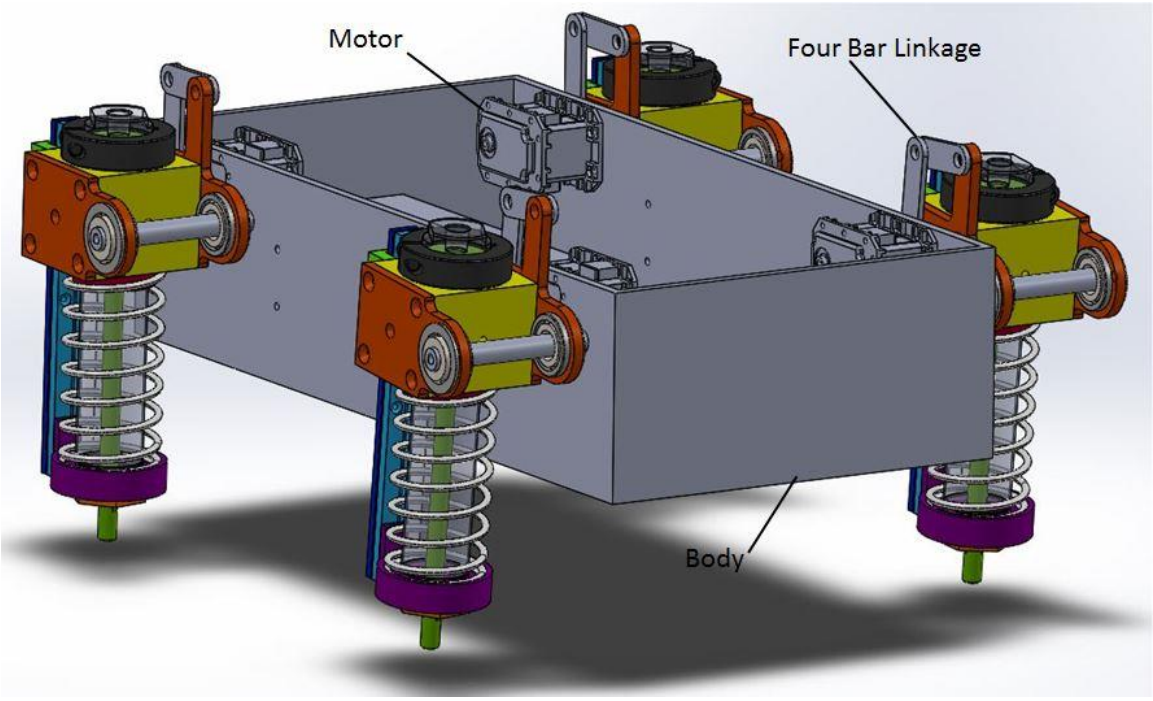

Figure 5.25: Leg design of the 4 DOF hopping robot.

To allow freedom of movement, the bearings and the slide rail of the one degree of freedom hopper are replaced with a bronze sleeve bearing installed inside the hip. This allows the cylinder and the hip to slide freely past one another. One end of the spring sits snugly inside the hip. The other end of the spring is pressed against the spring retainer which is fixed to the bottom of the cylinder. The result is that as you push down on the hip, the spring compresses and the sleeve bearing and hip move together along the shaft of the cylinder. When force is removed from the spring, the spring returns the hip to the original position.

The following custom parts were either machined aluminum or built using a rapid prototype printer: body, leg axles, hip, hip retainer, outer and inner linear strip plates, linear strip bracket, spring retainer, and the four bar linkage links. All parts were made with 6061 aluminum except for the acrylic inner linear strip plate and the polymer linear strip bracket.

A lever arm was added to the hip retainer to create a four bar linkage with a servo motor to allow for angular displacement of the leg with respect to the body. The four bar linkage system can be seen in Figure 5.25. This brought the degree of freedom in the robot to eight, however it was later discovered that once assembled, the robot was too heavy for the Dynamixel RX-28 motors, therefore the linkages were eventually fixed in place.

The actuators are Numatics M Series 1-1/16" spring return and are deployed using Numatics LO1 Series valves. The valves were mounted to the side walls of the body, positioned in between the motors.

The original design for control of the robot was with the Cerebot MC-7 board which uses a Microchip Pic-33 microcontroller. This was eventually changed to an Advantech PC-104. The digital input and output uses a Sensoray 526 board. The PC-104

was eventually chosen because of its ability to read in four encoders simultaneously. Figure 5.26 shows the component block diagram for easy visualization of the quadruped robot system.

Power was supplied by an 11.1 V and a 14.8 V battery. The 14.8 V battery could be used to power the motors. This was within the recommended applied voltage. Both batteries were connected in series adding the voltage to supply the 24 V solenoid valves for the actuators and the PC-104 power distribution board built by SpringActive. The power distribution board required a minimum of 25 V. Because of this requirement, the batteries were

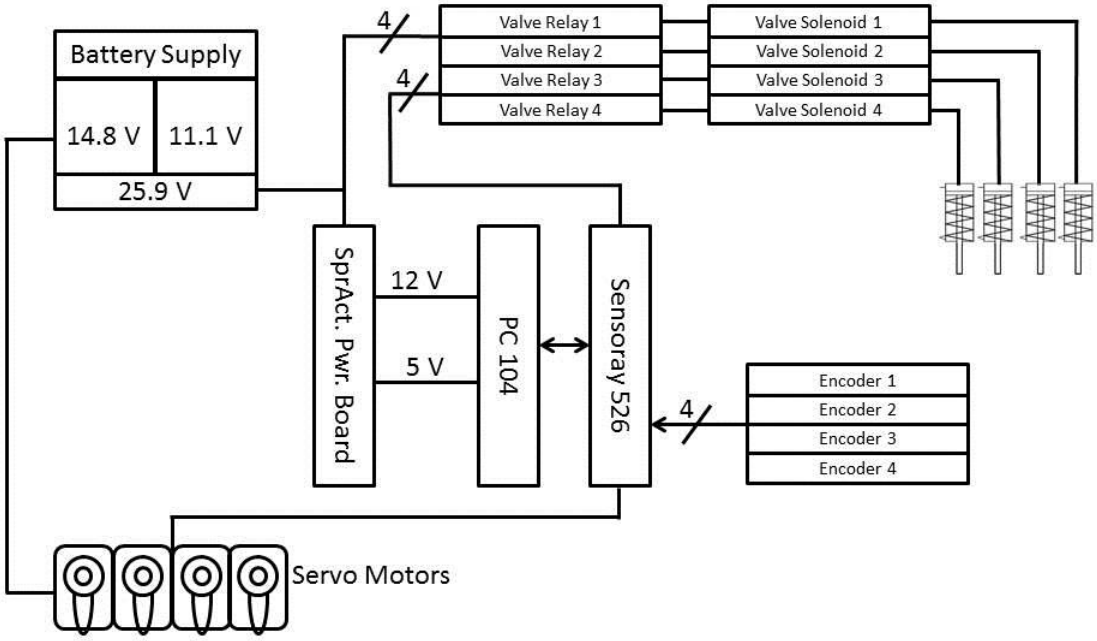

Figure 5.26: Block diagram showing component configuration of the quadruped system.

typically charged to 11.4 V and 15.1 V resulting in 26.4 V supply. This was the maximum recommended voltage for the solenoids. The Spring Active power distribution board maximum voltage is unknown but thought to be over 32 V.

5.2 SIMULATED VS. ACTUAL RESULTS

A 2 DOF planer Working Model was used to simulate how the quadruped might act. The model consisted of two spring actuator legs connected by a bar that acted as a link representing the longer side of the robot. The legs were fixed in a perpendicular position relative to the body.

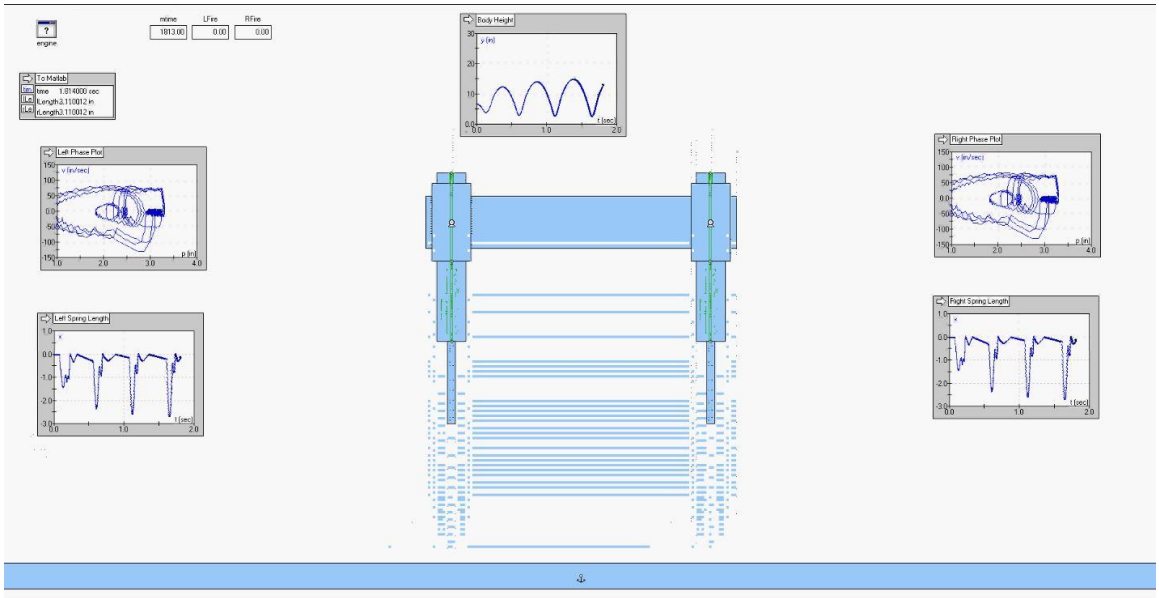

Figure 5.27: Working model simulation using two encoders to independently control each leg.

Some of the model parameters remained constant across all the simulations. These parameters are: total weight equal to 3.16 kg, spring constant of 1.23k N/m, and a spring length of 8.26 cm, and the center of mass sits 13.97 cm above the ground.

Four simulations were run to provide an estimate of what the robot might do in experimentation. One test was run with the actuators operating independently based on the phase angle of each leg. The applied force was 44.48 N per actuator, and the damping rate was 1.1 N/m. These values were based on the experimental and simulated results from the one degree of freedom hopper. The results of the simulation are shown in the Figures 5.28 through 5.35.

The phase portraits of the legs in Figures 5.28 and 5.29 shows that the controller produces a defined limit cycle. There is a visible amount of noise in the steady state portion of the plot. The steady state is represented in the graph by the dark band around the plot. The wider the band, the less the steady state converges to a singular value but rather to a range of values. In video representation of the simulation it can be seen that as the robot is hoping there are oscillations of the legs with respect to the body. This happens while both in the flight phase and while still in the stance phase but after the actuator has begun to fire. It is assumed that this phenomenon is what has created the noise in the leg phase plots.

Because the dynamics of both legs were set equal to each other in the model, it was not unexpected that if laid on top of one another, the plots can be seen to be exactly the same plot.

Figure 5.30 shows the body height over time. It shows that the input force of 10 lbf is a large enough force to allow the robot to jump more than double its body's center of mass height. The plot also shows that even though there is a range of heights, the apex does not change more than 10% of the hop height.

Figure 5.31 shows the phase portrait of the body for this simulation. The graph takes the more familiar shape seen with the one degree of freedom robot. There are however some variances. In some areas there are non-smooth portions, and there is a small dip and large bump shortly after the flight phase begins. These phenomena are due to the oscillation of the legs with respect to the body.

A second simulation used the same parameters but activated in a master/slave fashion with the phase angle plot of the left leg controlling both the left and right actuator. The results for this simulation did not vary to any degree from the first simulation.

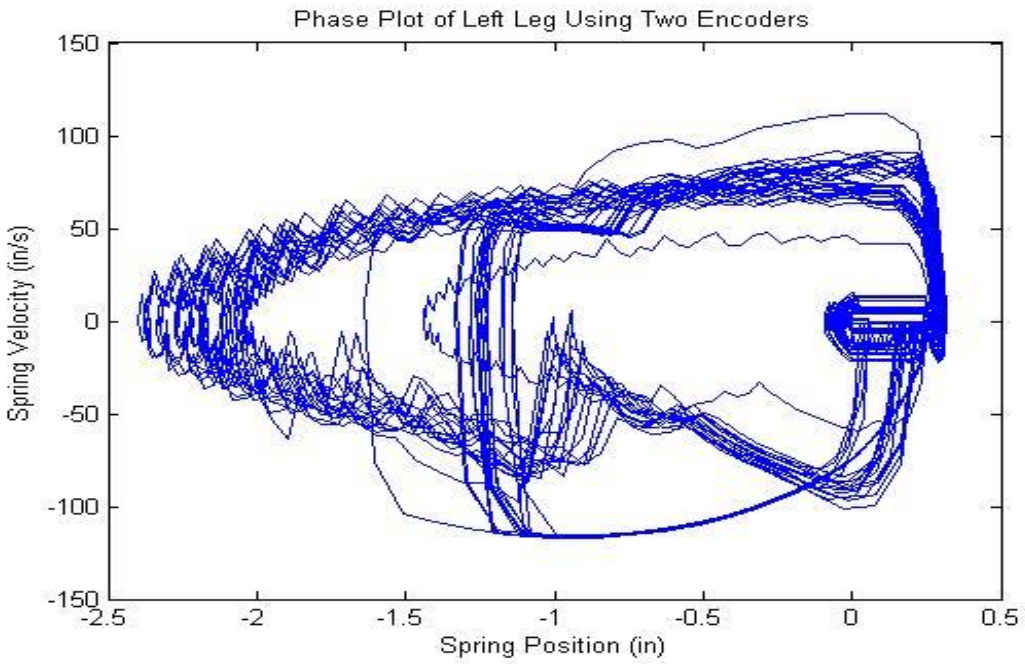

Figure 5.28: The simulated phase portrait of the left leg with individually activated actuators.

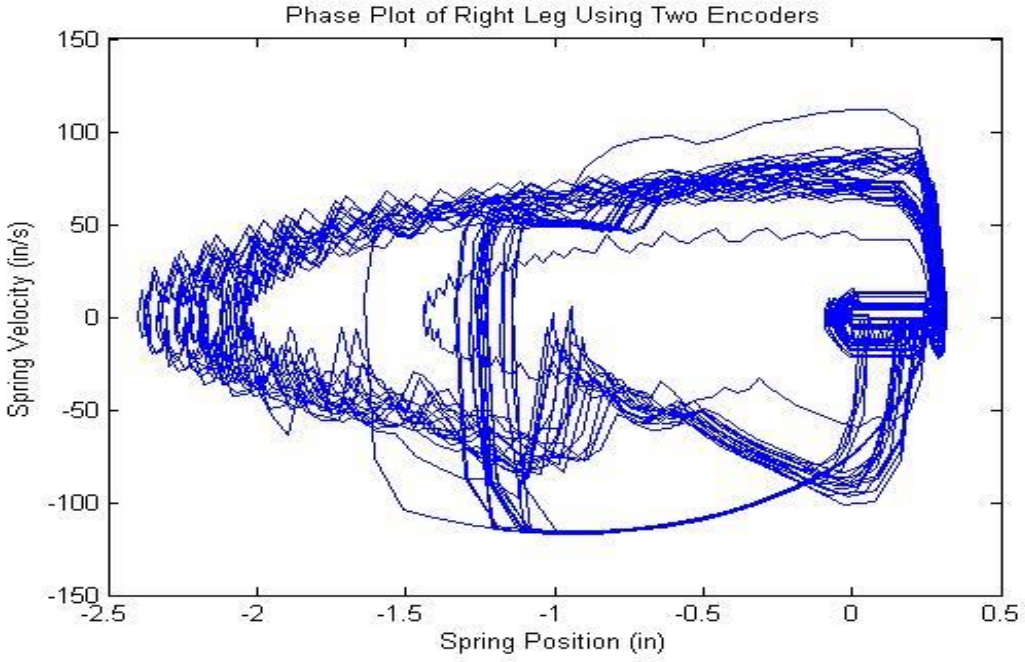

Figure 5.29: The simulated phase portrait of the right leg with individually activated actuators.

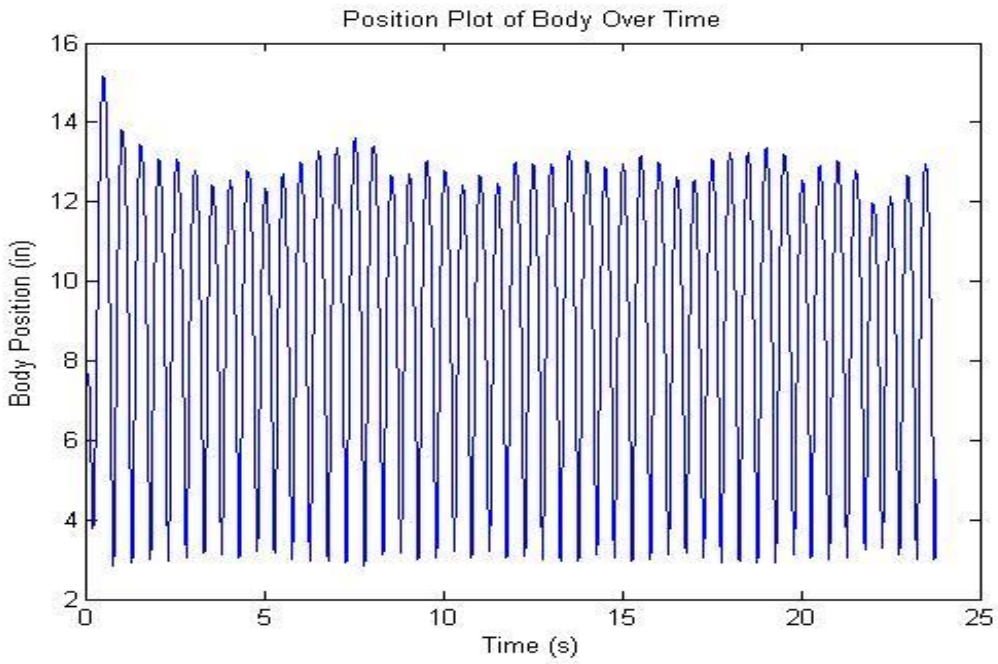

Figure 5.30: Graph of the body center of mass height over time while using two encoders.

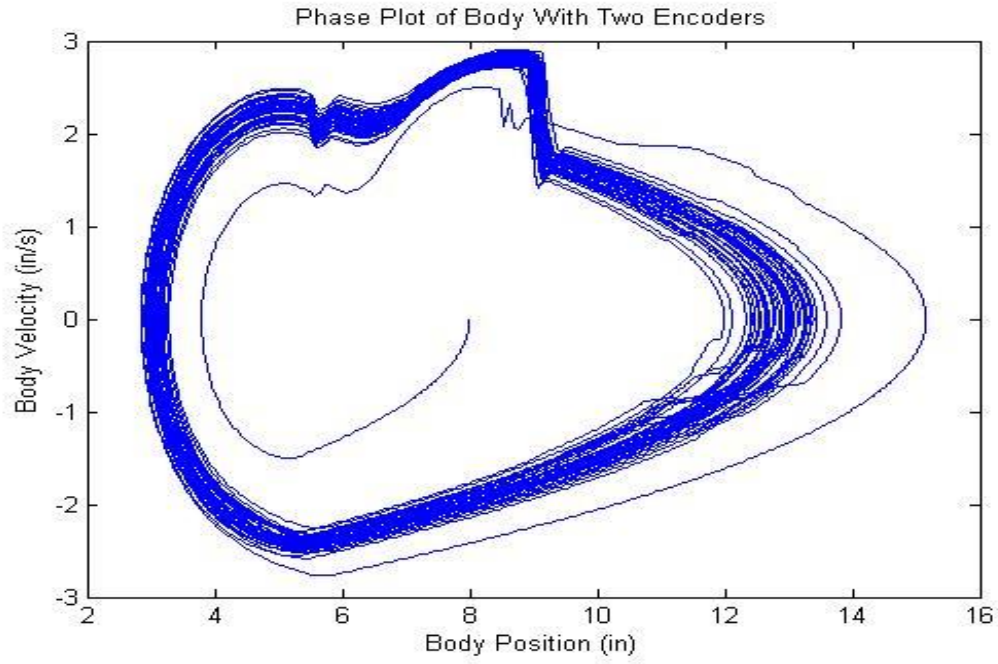

Figure 5.31: Phase portrait of the center of mass of the body while using two encoders.

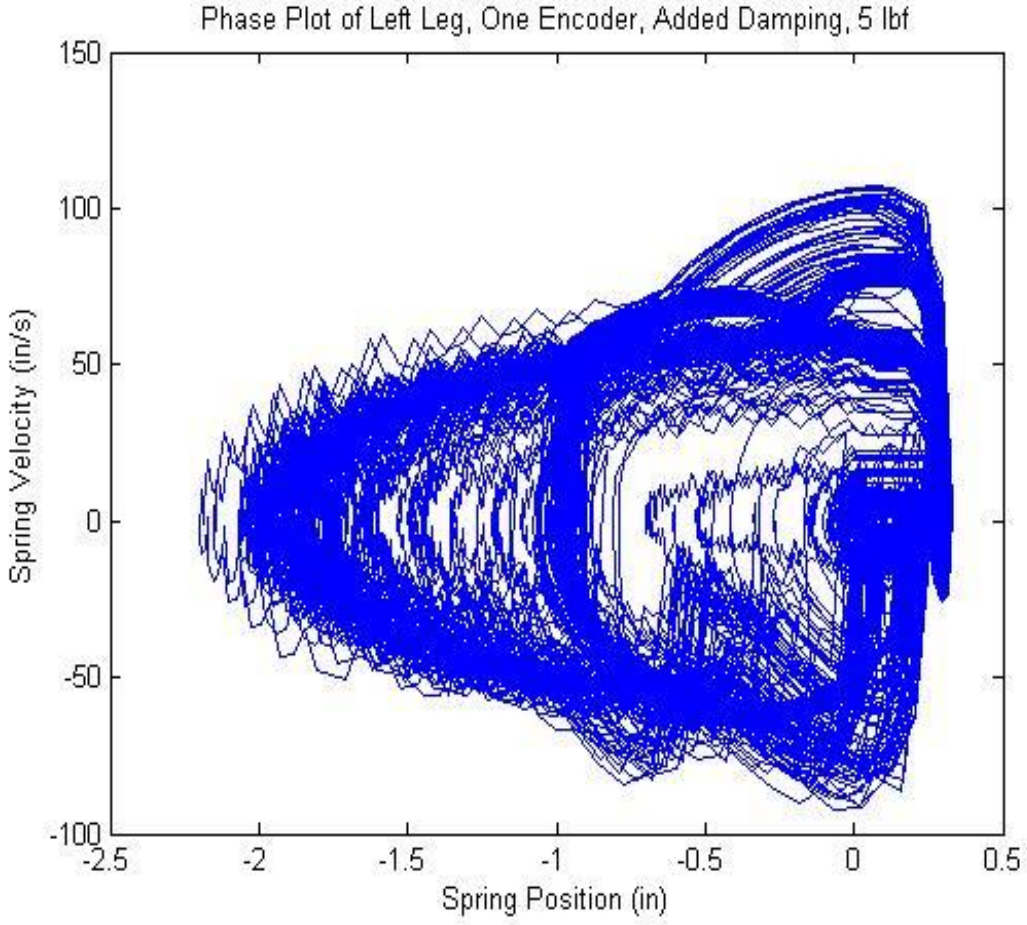

Figure 5.32: Phase portrait of the left leg with the reduced input force and a damping differential between the legs. The left leg was master to the right leg.

Because the results did not vary between the first two simulations damping was added to one leg to create a differential that would more appropriately reflect the real world. In this model, the damping of the left leg was reduced to 0.575 N/m and the right leg's damping remained at 1.1 N/m. The master/slave approach was used again. This resulted in an unstable hopping within the first few seconds of hopping.

As discussed above, the hop height was greater than double the body's center of mass. This hop height is much higher than needed to develop a limit cycle so another simulation was run with a reduced input force. The force that was 44.48 N per actuator

was changed to 22.24 N in hopes that by reducing the energy input the system would remain under control. Figures 5.32 to 5.35 shows the simulation response to the new energy input. In this simulation differences between the phase portraits of each leg begin to emerge as the legs fall into their own distinct limit cycle. It can be seen from the graphs that there is still heavy oscillation in the velocity presumably from the spring.

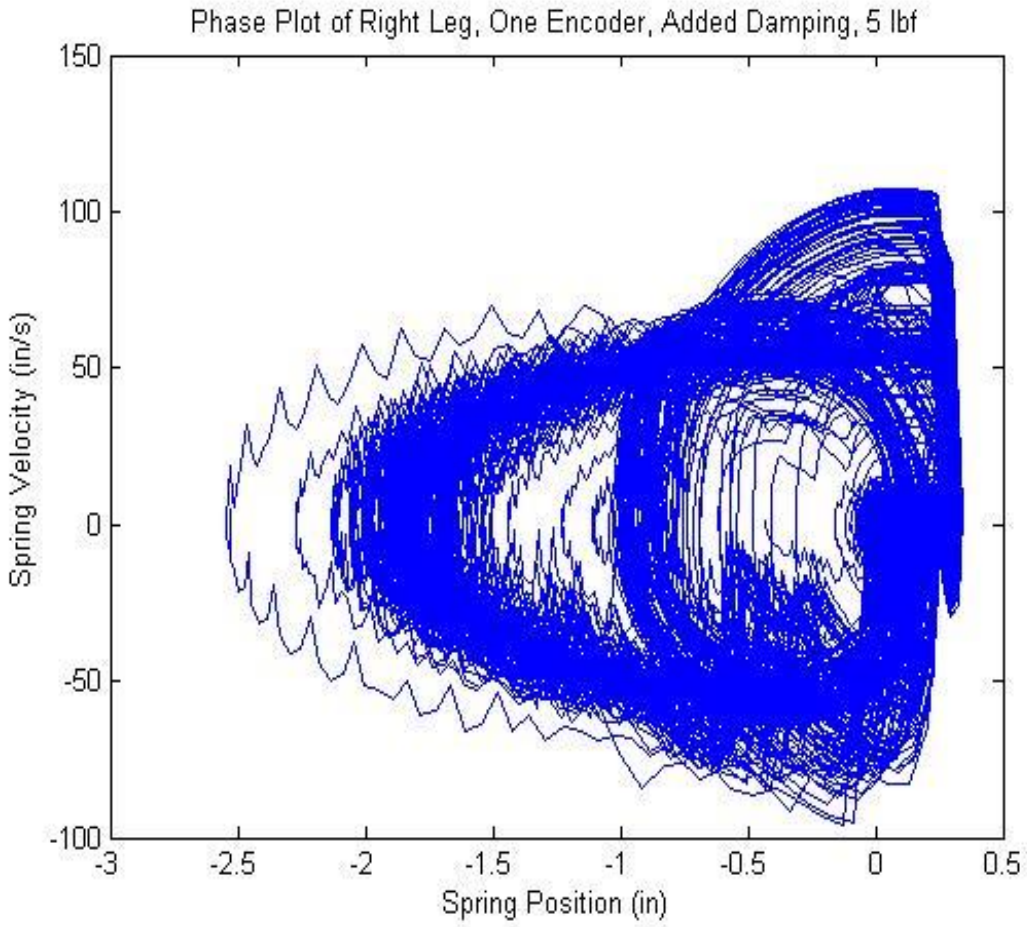

Figure 5.33: Phase portrait of the right leg with the reduced input force and a damping differential between the legs. The left leg was master to the right leg.

The overall trend of the profile, however, shows that the limit cycle exists within a narrow band. The darker appearance of Figures 5.32 through 5.35 is due to a longer

simulation time and therefore more data. Figure 5.35 shows the hop height of the body's center of mass over time. This simulation lasted 45 seconds to ensure that there was stability.

The body phase plot shows that the body is in the traditional limit cycle, albeit with some cycles that do not look very clean. While replaying the simulation it can be seen that the noisy traces happens around 39 to 42 seconds. This corresponds to two dips in the hop height graph of Figure 5.35. By the second 43, the robot was back to a stable hopping cycle.

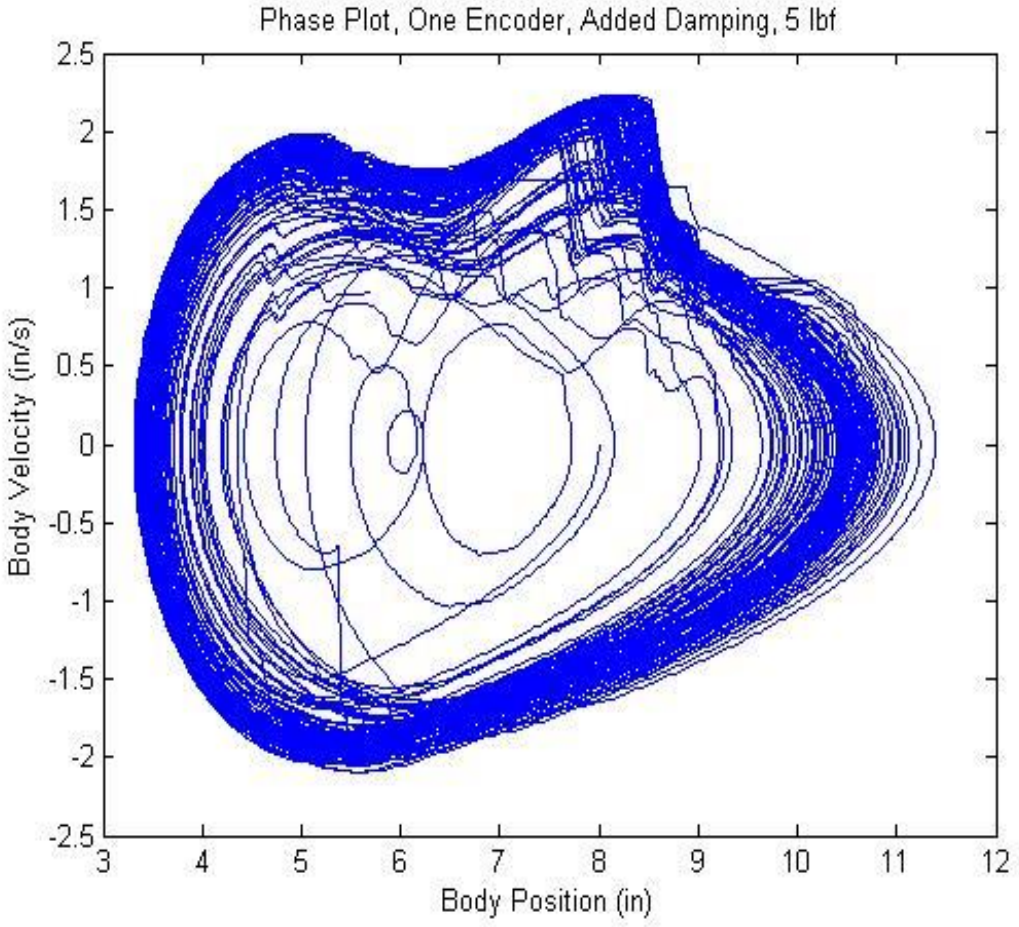

Figure 5.34: Phase portrait of the body's center of mass with the reduced input force and a damping differential between the legs. The left leg was master to the right leg.

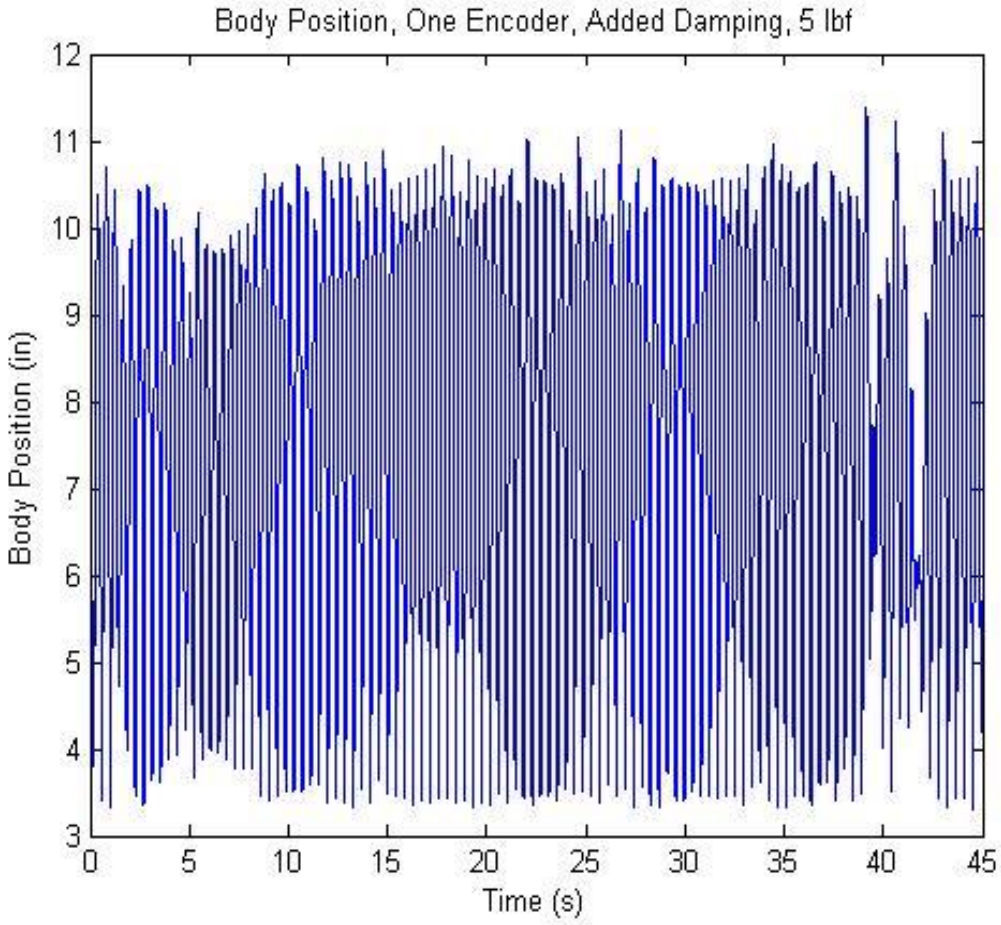

Figure 5.35: Hopping height of the body's center of mass over time, with the reduced input force and a damping differential between the legs. The left leg was master to the right leg.

Table 5.1: Testing schedule for the quadruped hopper. The cells marked represent the tests that were completed before the quadruped was damaged.

Quadruped Hopper	Transient Response	Steady State	Disturbance
One Encoder	X	X	X
Leg 1 and 3 Encoders			
Leg 1 and 4 Encoders			
All Encoders	X		

The robot was used to collect four sets of data, see Table 5.1. Three sets were collected using one encoder to determine when to activate all the actuators. All four

encoders collected position data. The fourth trial used all four encoders to determine the actuation timing of each individual, respective leg. Again, all four encoders collected position data for each leg.

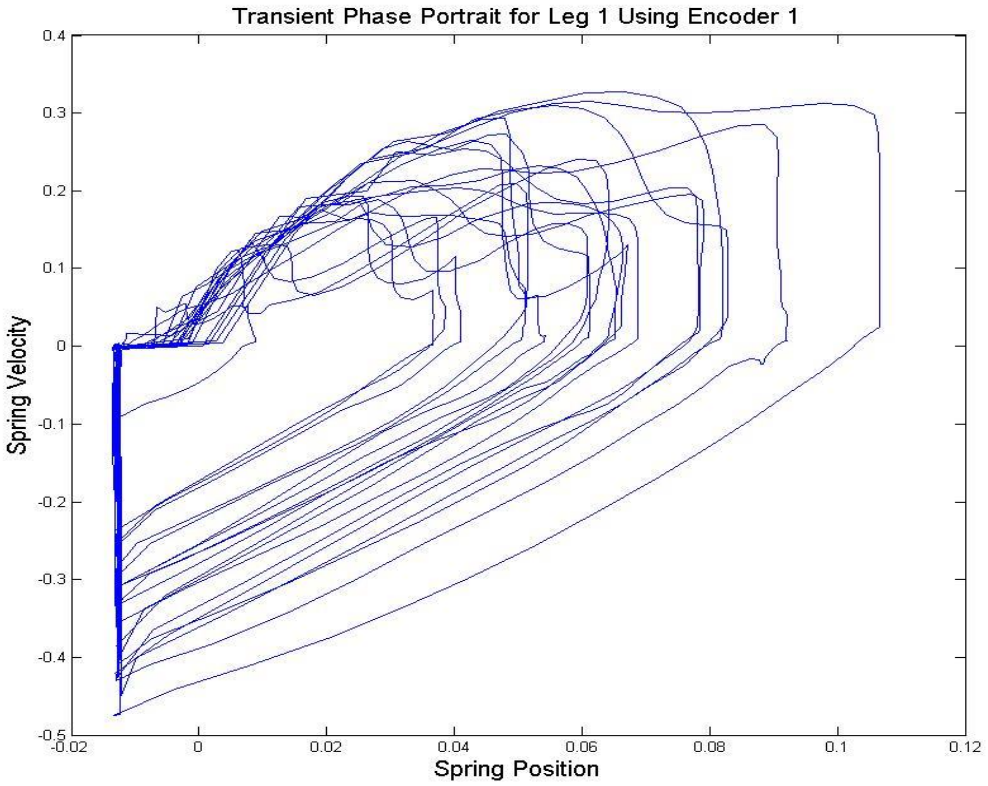

Figure 5.36: Transient phase portrait of leg 1 while actuation was controlled from this phase plot.

The phase portraits for the spring show that while the robot moved toward a steady state oscillation there were some full compressions of the springs. Approximately 0.15m represented a full compression of the spring. These events were the extreme case and were generally damped on the subsequent hops. There is a substantial variation in cycles during the recorded trial. Although there appears to be what one might call noise in Figure 5.36, a clear cycle emerges from the graph.

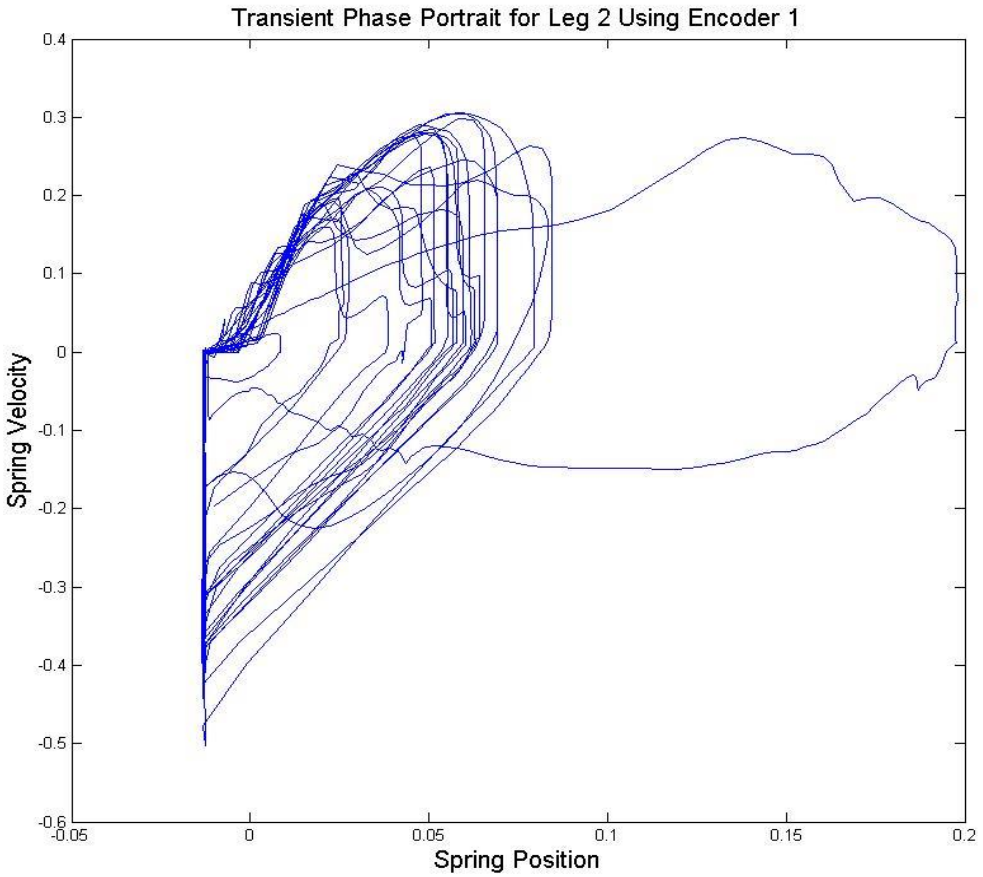

Figure 5.37: Transient phase portrait of leg 2 while actuation was controlled from the phase plot of leg 1.

In a video of the hopper, it appeared that the robot would get into a quasi-steady state but then "pop out" only to settle in again. This phenomenon could be seen over and over again.

In Figure 5.37, the loop that extends is inaccurate as it exceeds the amount of travel available in the spring. In all four transient phase portraits, Figures 5.36-5.39, the cycle is clearly defined and the maximum compression is assumed to have taken place. Similar to Figure 5.37, Figure 5.39 shows a cycle that is outside of the boundary of the maximum spring compression distance.

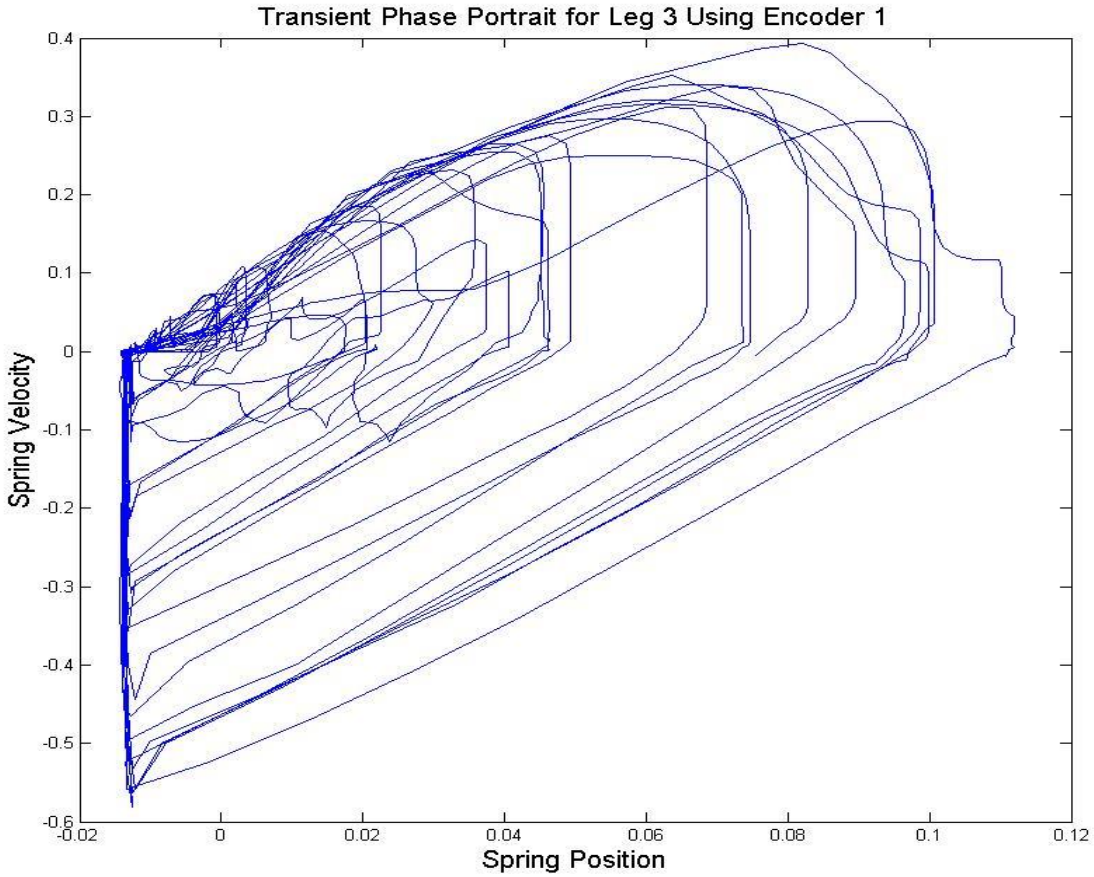

Figure 5.38: Transient phase portrait of leg 3 while actuation was controlled from the phase plot of leg 1.

It should also be noted that the spring compression did not follow a regular, increasing pattern. The compressions increased or decreased due in largest part to attitude of the robot. When a leg was the first to return to the ground, that particular leg would tend to compress more than the others. The last leg to hit was conversely the leg that experienced the least compression in its spring.

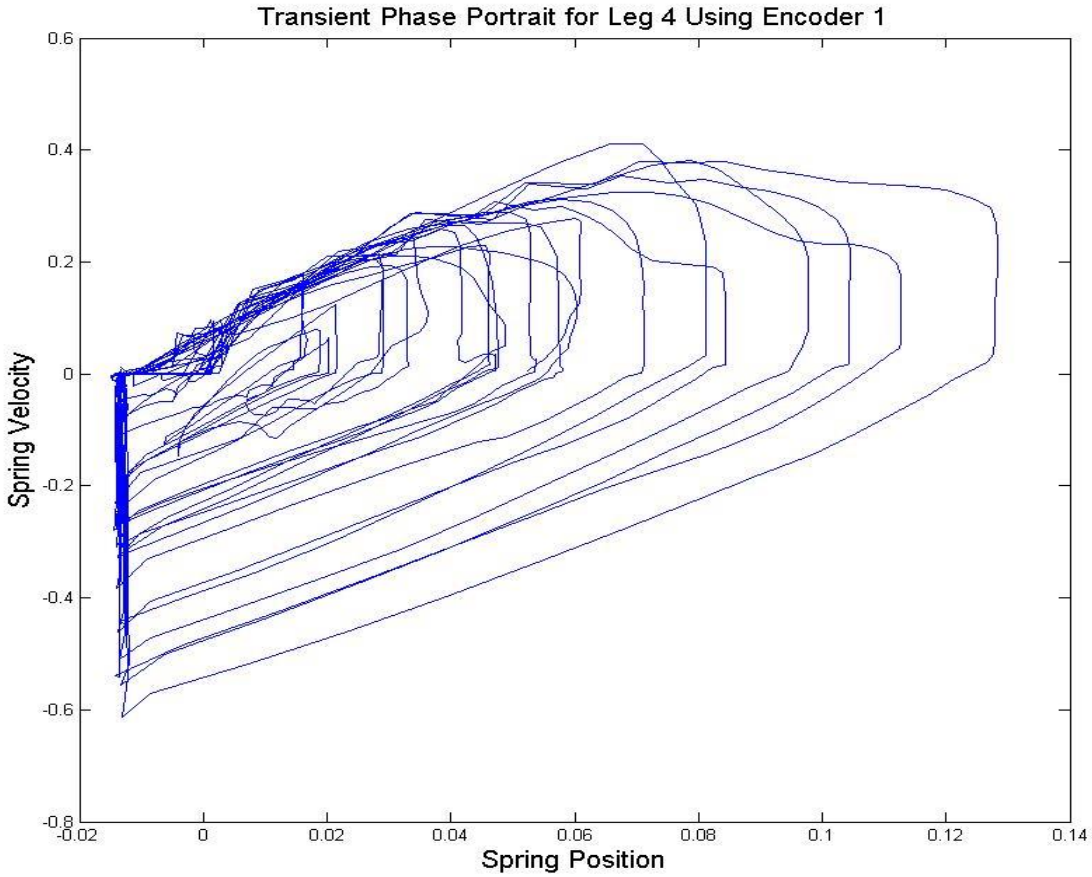

Figure 5.39: Transient phase portrait of leg 4 while actuation was controlled from the phase plot of leg 1.

Figures 5.40-5.43 represent the best approximation of a steady state. Even in this best case data there was a significant range in compression. This variance was again due to the orientation of the robot's body with respect to the ground. Leg 1 seems to have the tightest profile. This is likely due to its role as the actuator with the deterministic encoder.

At this point in the testing, the axles connecting the legs to the body had become bent. As a consequence the legs no longer allowed the take off into the flight phase to be normal to the ground. Figure 5.42 shows the robot after the deformation occurred. The

leading factor in the absence of a clearly defined steady state in the testing may have been the addition of the unintended dynamics introduced by the skewed legs.

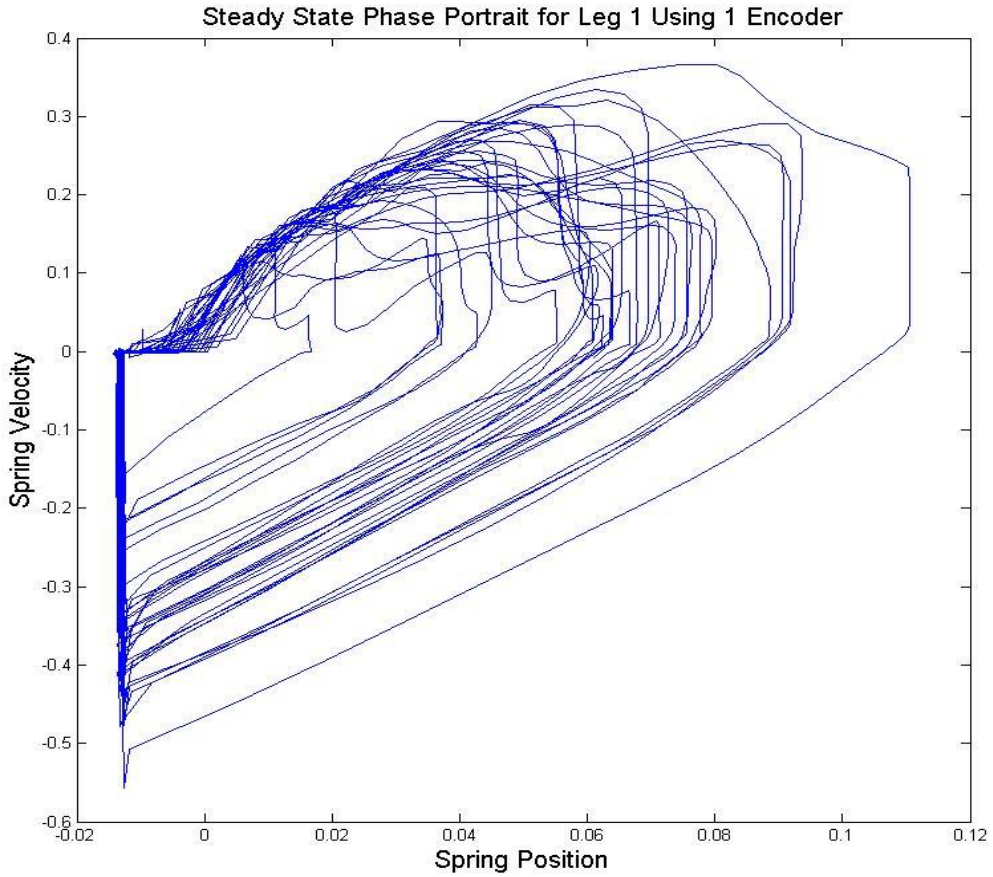

Figure 5.40: Steady state phase portrait of leg 1 while actuation was controlled from the phase plot of leg 1.

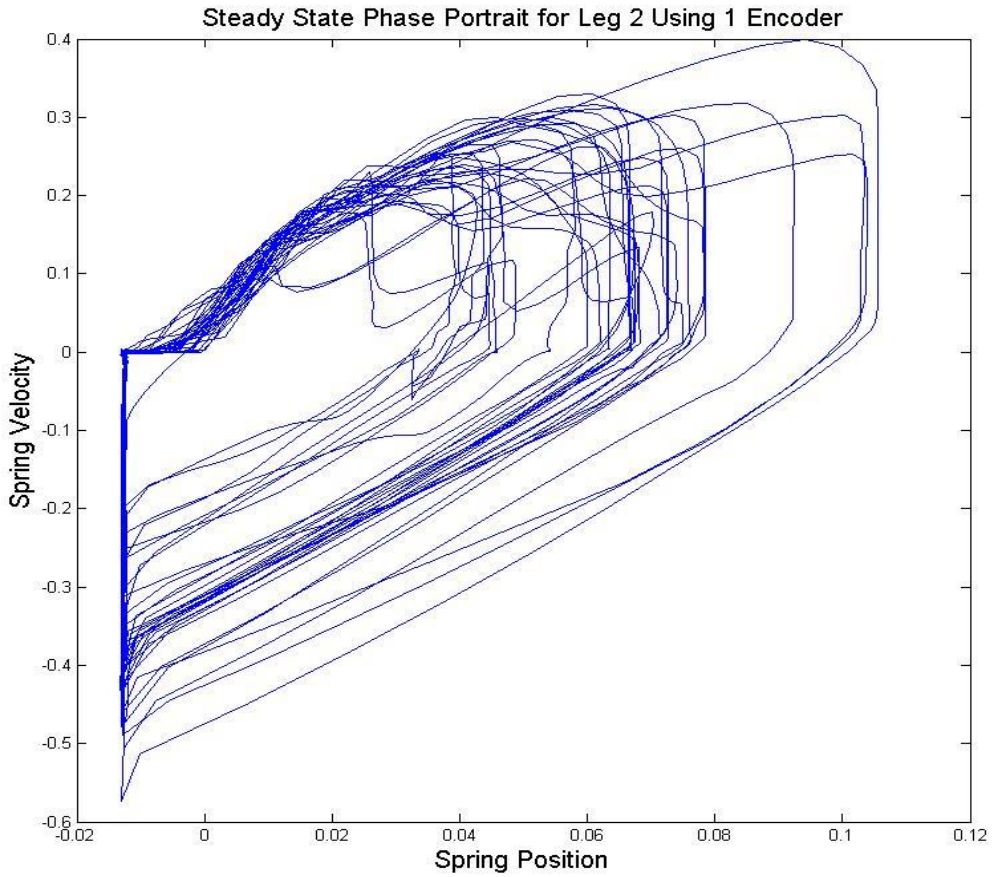

Figure 5.41: Steady state phase portrait of leg 2 while actuation was controlled from the phase plot of leg 1.

Figures 5.40 and 5.41 have the better representations of a steady state. The concentrated bands in legs one and two allude to the possibility of consistent hopping. These two legs are attached to the least bent axles giving additional reason to believe that the angle of thrust is critical to the dynamics when each leg is independently controlled.

Figures 5.42 and 5.43 represent legs 3 and 4. It takes a much greater imagination to see a pattern that could represent steady state in these phase plots.

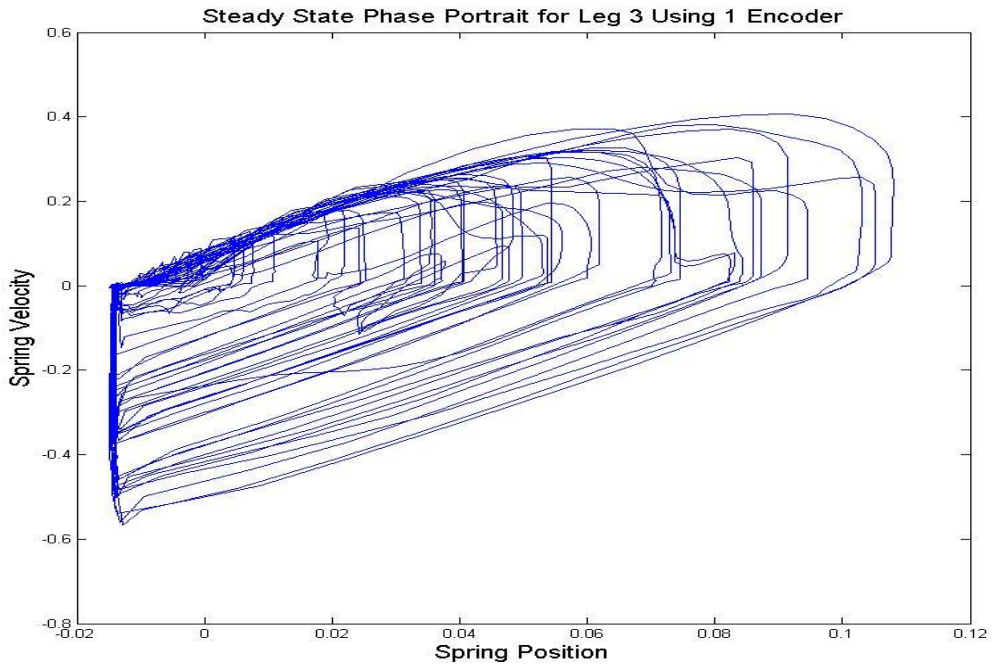

Figure 5.42: Steady state phase portrait of leg 3 while actuation was controlled from the phase plot of leg 1.

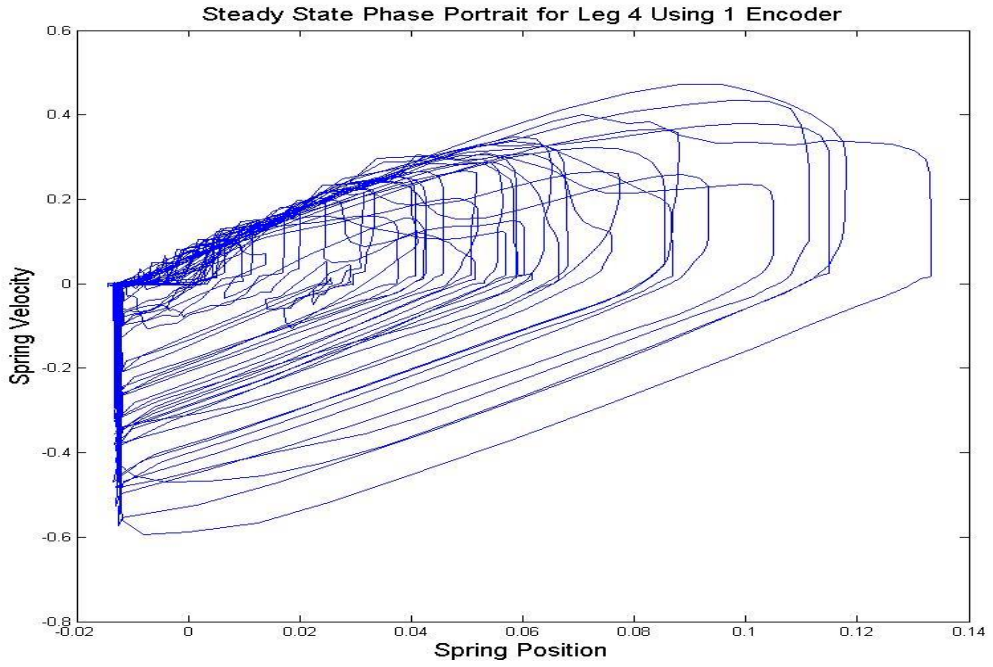

Figure 5.43: Steady state phase portrait of leg 4 while actuation was controlled from the phase plot of leg 1.

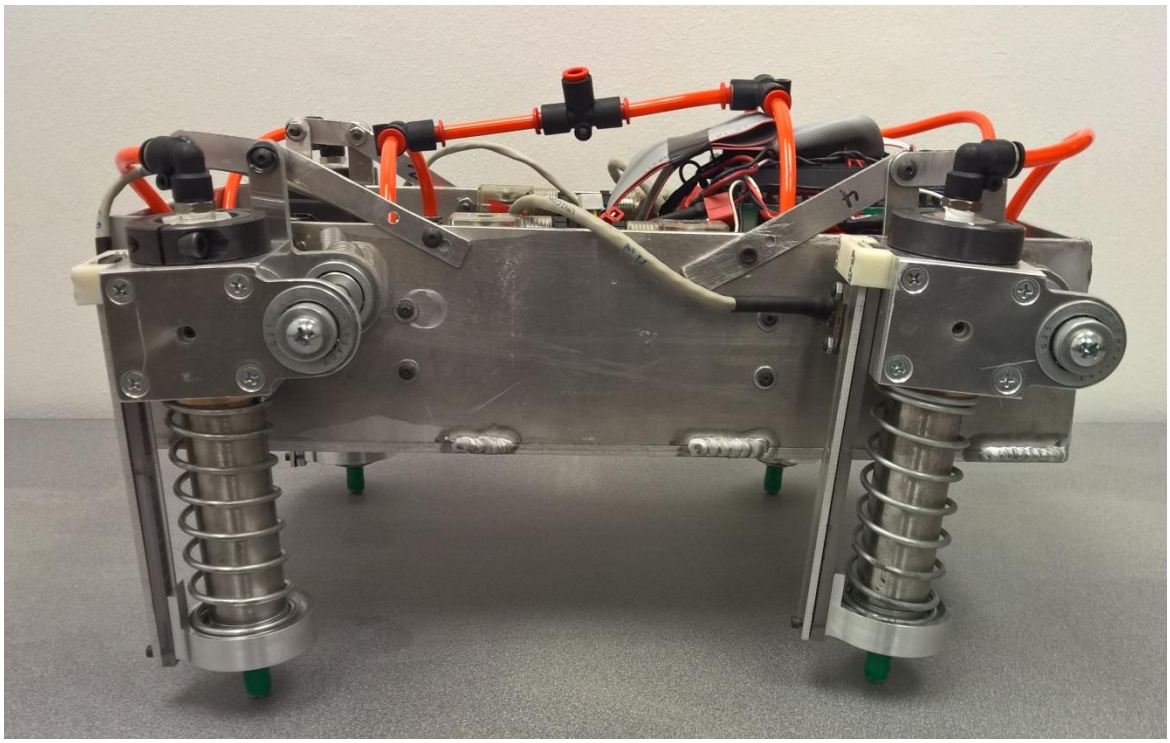

Figure 5.44: After hopping many cycles, the axles supporting the legs began to bend creating an unintended leg angle.

Figures 5.45 through 5.48 displays the test results from a trial that introduced a disturbance. It is difficult to see the disturbance in these profiles because as in the other plots the noise is larger than the disturbance itself. It should be noted that the bending in the axles was progressive with the trials. Since the disturbance was created by manually nudging or hitting robot while hopping, a disturbance may have had the effect of correcting the attitude of the robot more than disturbing it in some instances.

It again appears that legs 1 and 2 resemble something similar to a steady state with darker bands in the cyclical plot. This illustrates why it was earlier called a quasi-steady state.

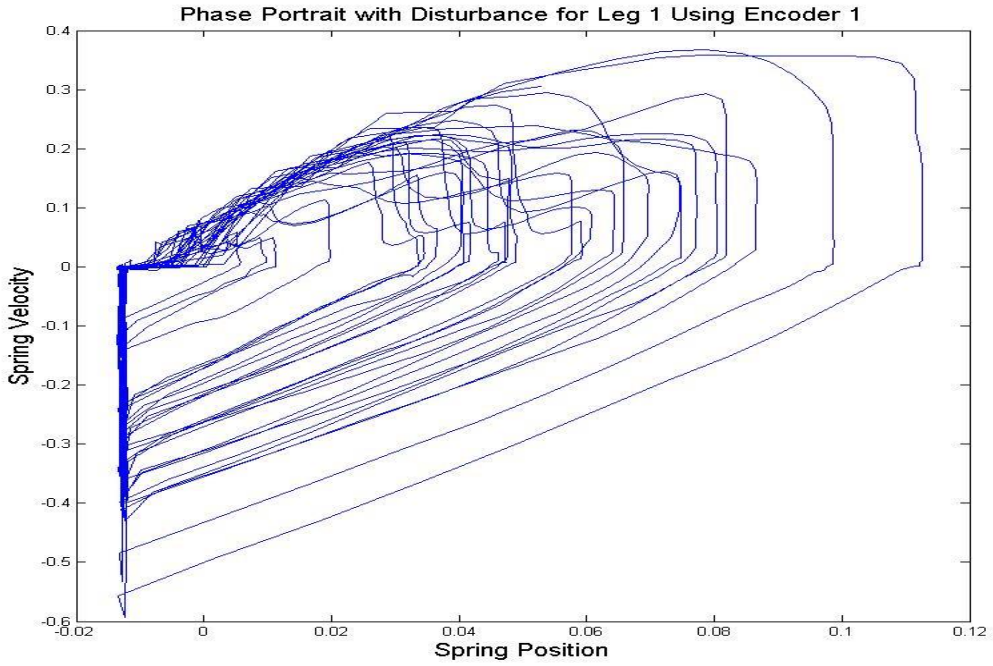

Figure 5.45: The phase portrait of leg 1 with an added disturbance while actuation was controlled from the phase plot of leg 1.

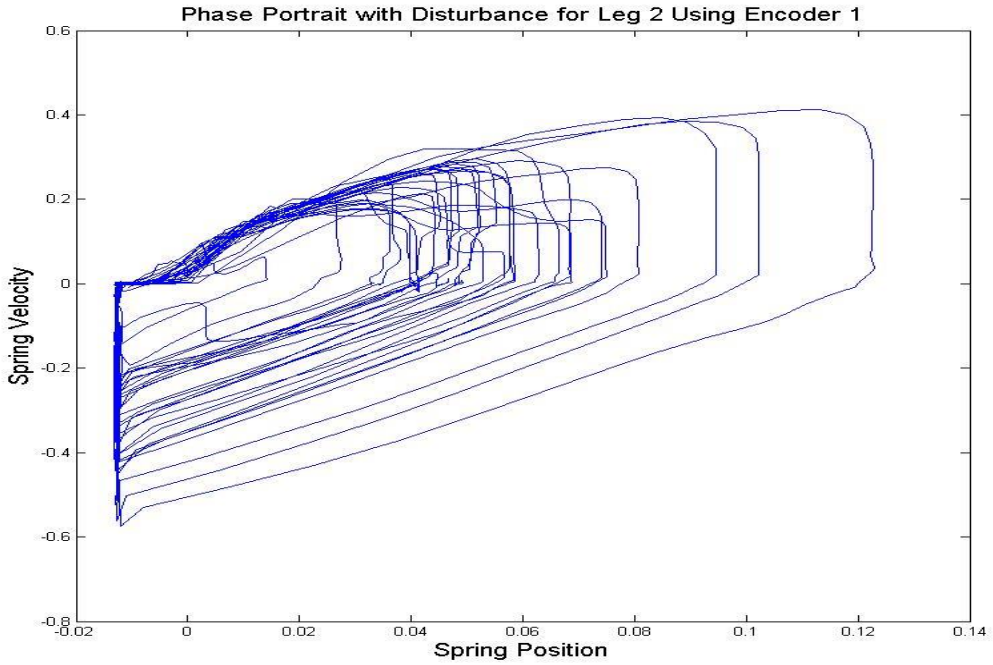

Figure 5.46: The phase portrait of leg 2 with an added disturbance while actuation was controlled from the phase plot of leg 1.

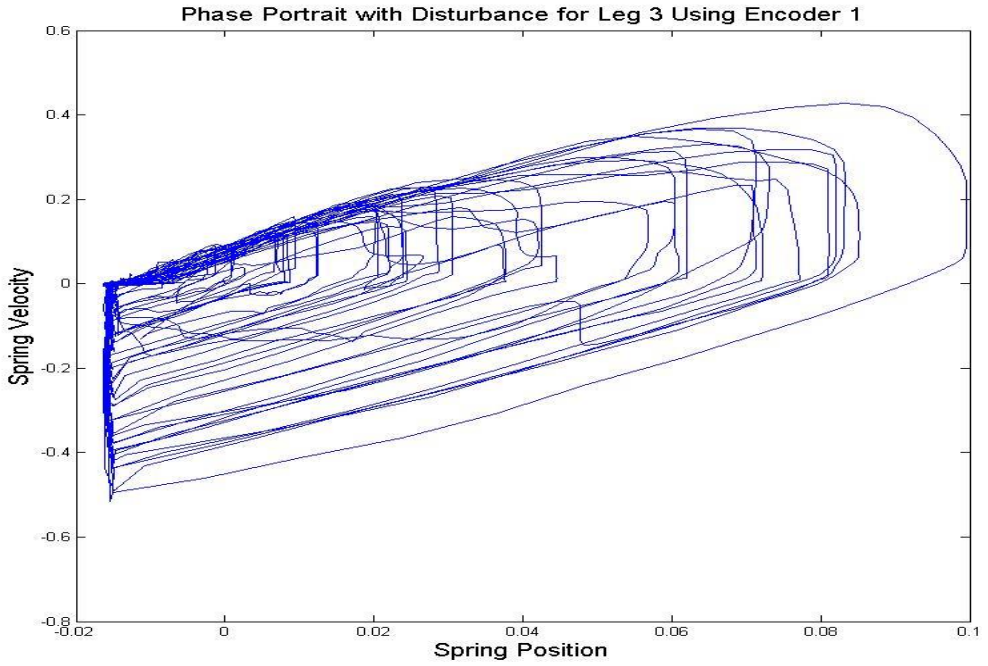

Figure 5.47: The phase portrait of leg 3 with an added disturbance while actuation was controlled from the phase plot of leg 1.

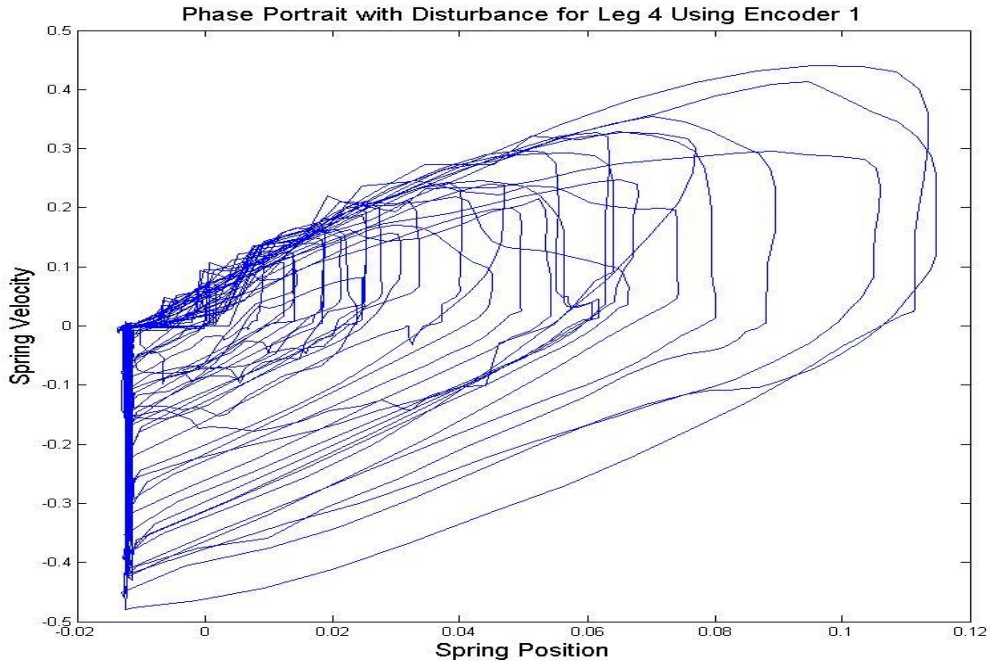

Figure 5.48: The phase portrait of leg 4 with an added disturbance while actuation was controlled from the phase plot of leg 1.

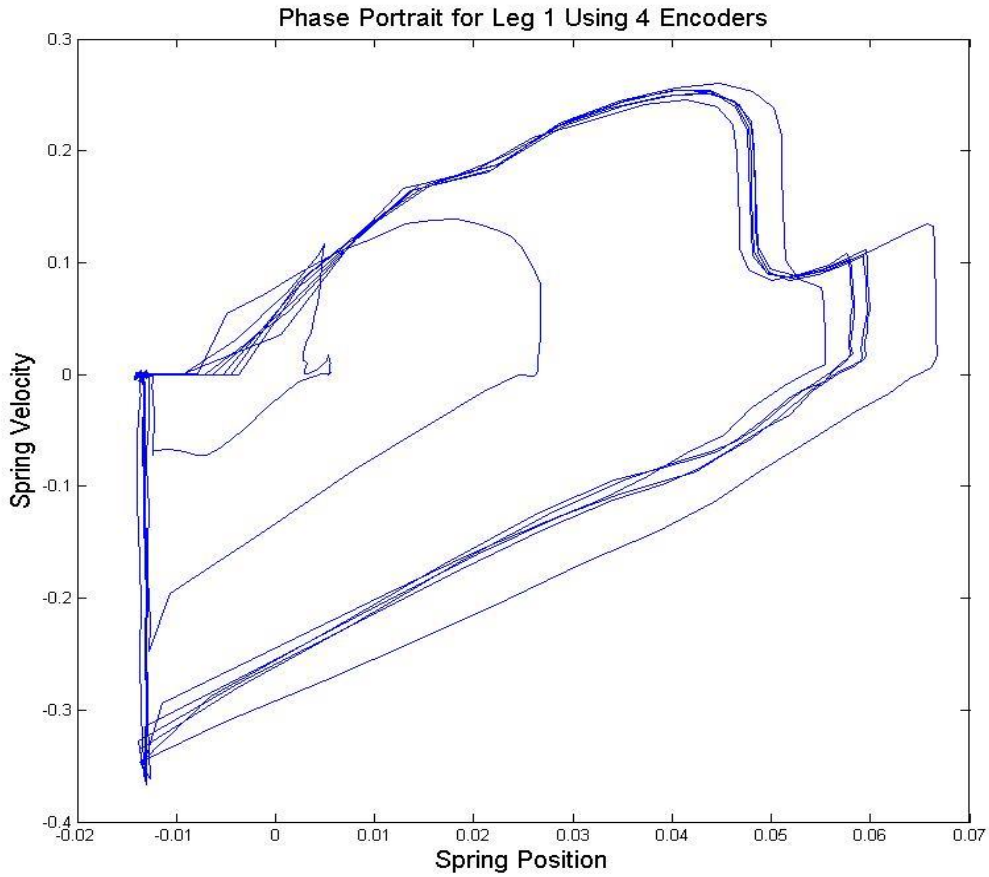

Figure 5.49: The phase portrait of leg 1 with an added disturbance while actuation was controlled from the phase plot of each individual leg.

The final trial in which all four encoders were used to independently actuate the legs, we see the most variety in profiles between each leg. It is also apparent from Figures 5.49 through 5.52 that there are fewer cycles in this trial than in all the other tests. In this mode, the robot quickly became unstable and flipped over and was then unable to hop without being manually righted. This test set up was run three times with the essentially the same result of the robot flipping upside-down. This ended each try.

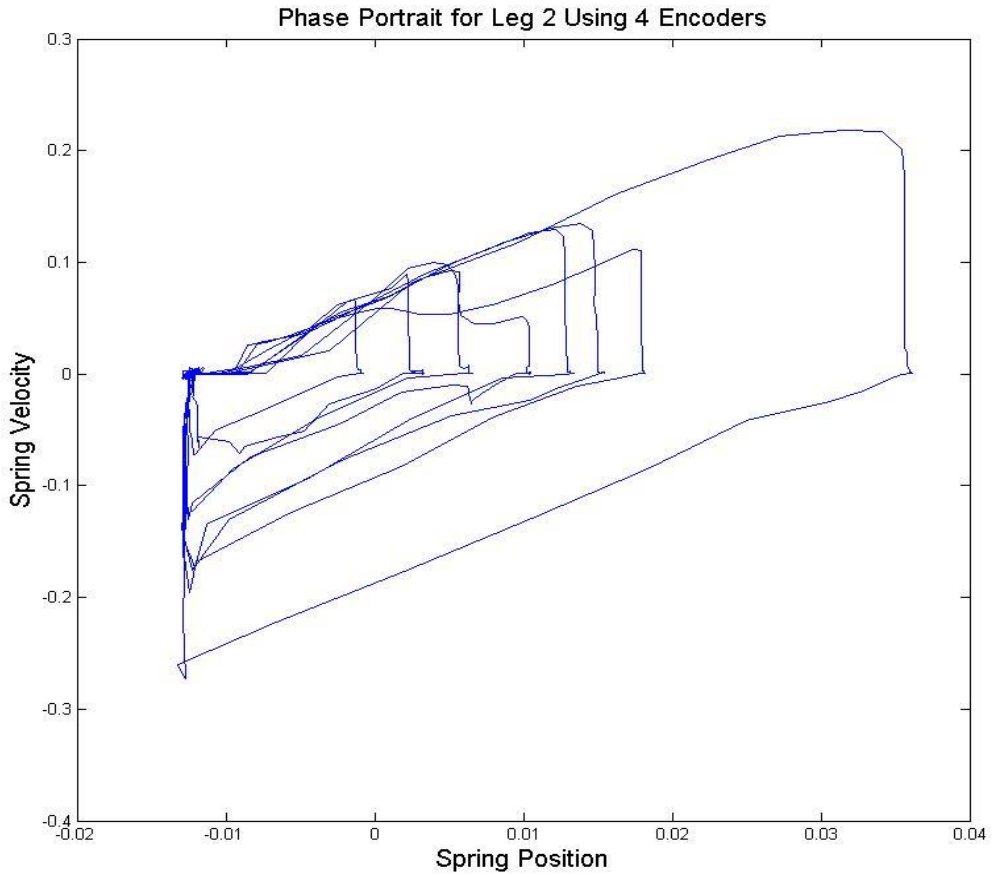

Figure 5.50: The phase portrait of leg 2 with an added disturbance while actuation was controlled from the phase plot of each individual leg.

It is hard to develop any meaningful conclusions from this last trial. It seems that legs 2 and 3 were having difficulty getting very far off the ground and 1 and 4 were getting the better hop heights. This was a bad combination because legs 1 and 4 were on one side of the robot and legs 2 and 3 were on the other. This difference lends itself to flipping as was witnessed.

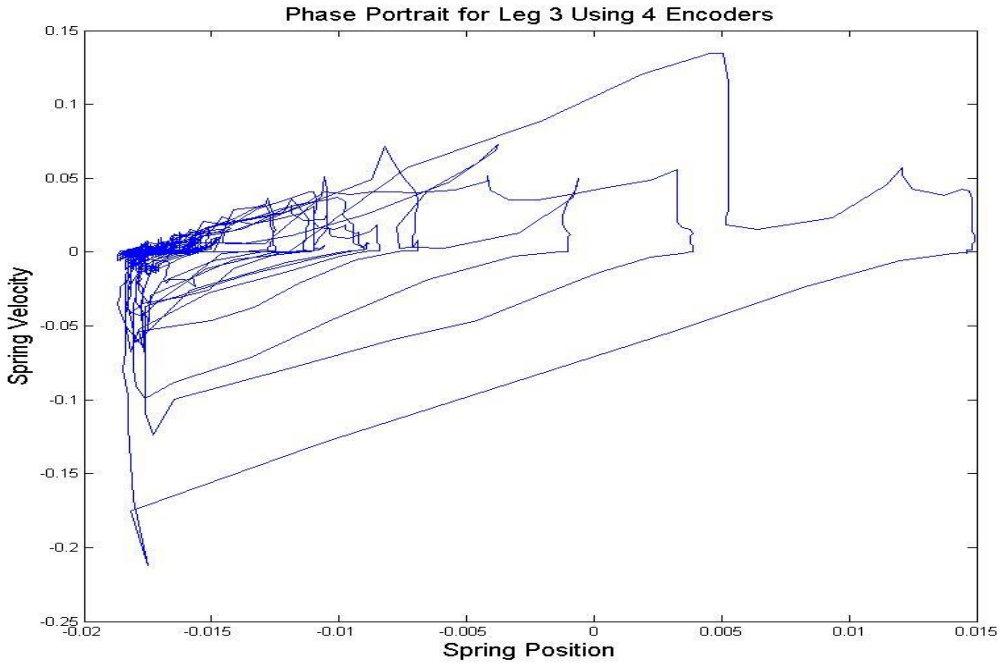

Figure 5.51: The phase portrait of leg 3 with an added disturbance while actuation was controlled from the phase plot of each individual leg.

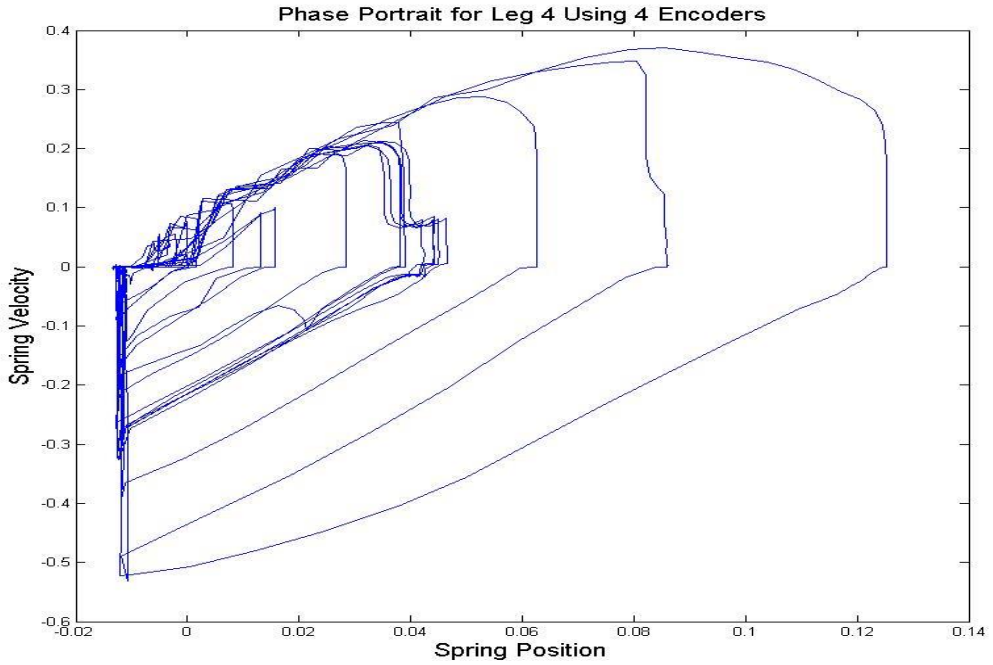

Figure 5.52: The phase portrait of leg 4 with an added disturbance while actuation was controlled from the phase plot of each individual leg.

Chapter 6

CONCLUSIONS, GAIT STRATEGIES AND FUTURE WORK

The simulations show that model was extraordinary in its capacity to emulate the one degree of freedom hopper. The robot proved that the phase oscillator controller can produce a terrain following hopper that is robust when faced with a breadth of initial conditions or disturbances.

Future work for this hopper would be to further tune the simulation parameters to produce an even better match to experimental data. It was shown that damping could be added to the system by activating out of phase with the system. It would be interesting to learn more about the relationship of the phase angle activation to damping. If the amount of damping could be accurately controlled by the angle of activation, an algorithm could be developed to help stabilize multi-legged hoppers by adjusting the damping on the fly.

Four gait strategies were planned for testing on the quadruped robot. The first was using a single encoder to create the deterministic phase profile for all four actuators. A second strategy was to use one encoder from each of what was considered to be the front and back, or the more distant ends of the robot. The third strategy was to use one encoder from the left side and one from the right side of the robot. The final strategy was to use all four leg profiles independently.

Due to mechanical issues that began to develop as testing went on, only two of the desired strategies were tested. Of the two strategies, only one was fully explored in the sense that data was collected on the transient response, a steady state phase, and the response to a disturbance.

The test results showed that the quadruped responded much better to feedback input from only one encoder. It is difficult to say at this time if this is due to anything

other than insufficiencies in the quadruped itself. The simulations, however, seem to indicate that when dynamics are equal in each leg, the robot can produce stable limit cycles. It is possible that if work on the one degree of freedom robot were to successfully uncover a good method for damping control that type of method could potentially help to stabilize a quadruped with imbalances.

As for future work, it would be interesting to see the quadruped legs on a redesigned body that had reinforcement on the axles. Attaching each end of the axle to a support would be a great improvement over the cantilever style on this quadruped.

Another improvement to the quadruped that would benefit both the reduction of stress on the axles and the motors would be to concentrate on a reduction of weight. The most significant part to be redesigned to that end would be the body. I would suggest that one solution is that a simple frame be built from aluminum extrusions rails.

REFERENCES

[1] Naidoo, Y., Stopforth, R., and Bright, G., 2011, "Development of an UAV for Search & Rescue Applications – Mechatronic Integration for a Quadrotor Helicopter," *AFRICON 2011* (pp. 1-6). IEEE

[2] Defense Advanced Research Project Agency (DARPA), 2013, "Digitizing SQUAD X: Sensing, Communications, Mission Command, and Soldier-worn Backbone," DARPA-SN-13-34, Accessed on 22 October, 2014 https://www.fbo.gov/index?s=opportunity&mode=form&id=3d6f0f8cb8cfe02a24a8d849c6cb33dc&tab=core&_cview=1

[3] Nelson, G. 2015, "Where is Google's Car Going?" *Automotive News,* **89** (6654), pp 1. Accessed on 12 February, 2015 http://login.ezproxy1.lib.asu.edu/login?url=http://search.proquest.com/docview/1643217848?accountid=4485

[4] Hong, D.W. 2002, "Analysis and Visualization of the Contact Force Solution Space for Multilimbed Mobile Robots," Ph.D. thesis (Order No. 3099796). Purdue University, Lafayette, IN Accessed on 10 April, 2015 http://login.ezproxy1.lib.asu.edu/login?url=http://search.proquest.com/docview/305541916?accountid=4485

[5] Hong, D.W., Ingram, M., and Lahr, D. 2009, "Whole Skin Locomotion Inspired by Amoeboid Motility Mechanisms," *ASME Journal of Mechanisms and Robotics*. **1**

[6] Hong, D.W., and Cipra, R.J., 2006, "Optimal Contact Force Distribution for Multi-Limbed Robots," *ASME Journal of Mechanical Design*, **128**, (3) pp 566-573

[7] Sayyad, A., Seth, B., and Seshu, P., 2007, "Single-Legged Hopping Robotics Research - A Review," *Robotica*, **25**, pp 587-613

[8] Tokhi, M.O., Virk G.S., and HossainM.A., 2006, "Climbing and Walking Robots," *Proceedings of the 8th International Conference on Climbing and Walking Robots and the Support Technologies for Mobile Machines* (CLAWAR 2005). Springer Berlin Heidelberg.

[9] Wettergreen, D., Thorpe, C., and Whittaker, W.L., 1993, "Exploring Mount Erebus by Walking Robot," *Robotics and Autonomous Systems*, **11** pp. 171-185

[10] Murphy, R.R., 2004, “Trial by Fire [rescue Robots],” *IEEE Robotics Automation Magazine* **11**, (3) pp. 50–61

[11] Aguirre-Ollinger, G., Colgate, J. E., Peshkin, M. A., and Goswami, A., 2007, "A 1-DOF Assistive Exoskeleton with Virtual Negative Damping: Effects on the Kinematic Response of the Lower Limbs," IROS 2007, *IEEE/RSJ International Conference on Intelligent Robots and Systems*

[12] Holgate, M. A., Bohler, A. W., and Sugar, T. G., 2008, "Control Algorithms for Ankle Robots: A Reflection on the State-of-the-Art and Presentation of Two Novel Algorithms," *Biomedical Robotics and Biomechatronics,. BioRob 2008. 2nd IEEE RAS & EMBS International Conference on*, 2008, pp. 97-102.

[13] Holgate, M. A., Sugar, T. G., and Bohler, A. W., 2009, "A novel control algorithm for wearable robotics using phase plane invariants," in *Robotics and Automation, ICRA '09. IEEE International Conference on*, pp. 3845-3850.

[14] Hogan, N. 1984, "Impedance Control: An Approach to Manipulation," in *American Controls Conference*, pp. 304-313.

[15] New, P., Wheeler, C., Sugar, T.G., 2014, “Robotic Hopper Using Phase Oscillator Controller,” ASME 2014 International Design Engineering Technical Conferences and Computers and Information in Engineering Conference, ASME

[16] Sugar, T.G., Bates, A., New, P., et al., 2015, “Limit Cycles to Enhance Human Performance based on Phase Oscillators.” Journal of Mechanisms and Robotics **7.1** (0110011) pp.1-8

[17] Raibert, Marc, 1986, “Legged Robots,” *Communication of the ACM*, **29**, (6) pp. 499-514

[18] Nof, S.Y., 1999, *Handbook of Industrial Robotics*. John Wiley, New York: pp. 148, Print

[19] Zhuang, H.C., Gao H.B., and Deng, Z.Q., et al. 2014, “A Review of Heavy-Duty Legged Robots,” *Sci China Tech Sci*, (57) pp. 298-314

[20] Carbone, G., and Ceccarelli, M., 2005, *Legged Robotic Systems*. INTECH Open Access Publisher: pp. 557-561

[21] Nelson, G., Blankespoor, K., and Raibert, M., 2006, "Walking BigDog: Insights and Challenges from Legged Robotics," Journal of Biomechanics **39** (Supplement 1) pp. S360

[22] Ma, J., Susca, S., and Bajracharya, M., et al. 2012, "Robust Multi-Sensor, Day/Night 6-DOF Pose Estimation for a Dynamic Legged Vehicle in GPS-Denied Environments," *Robotics and Automation (ICRA), 2012 IEEE International Conference on*. IEEE

[23] Wilcox, B.H., 2009, "ATHELETE: A Cargo and Habitat Transporter for the Moon," *Aerospace Conference, 2009 IEEE*, IEEE

[24] Ishi, H., Koga, H., and Obokawa,, Y., et al., 2010, "Path Generator Control System and Virtual Compliance Calculator for Maxillofacial Massage Robots," *International Journal of Computer Assisted Radiology and Surgery*, **5** pp. 77-84

[25] Haeufle, D.B.F, Grimmer, and S., Seyfarth, A., 2010, "The Role of Intrinsic Muscle Properties for Stable Hopping – Stability is Achieved by the Force-Velocity Relation," *Bioinspiration & Bimimetics*, (5) pp. 1-11

[26] Zhou, X., and Bi, S., 2012, "A Survey of Bio-Inspired Compliant Legged Robot Designs," *Bioinspiration & Bimimetics*, (7) pp. 1-20

[27] Mochon, S., and McMahon, T.A., 1980, "Ballistic Walking: An Improved Model," *Mathematical Biosciences* **52** (3-4) pp.241-260.

[28] Formal'sky, A., Chevallereau, C., and Perrin, B., 2000, "On Ballistic Walking Locomotion of a Quadruped," *The International Journal of Robotics Research*, **19** (8) pp. 743-761

[29] Kalveram, K.T., Haufle, D., Grimmer, S., and Seyfarth, A., 2010, "Energy management that generates hopping. Comparison of virtual robotic and human bouncing," *Proceedings of SIMPAR 2010 Workshops. International Conference on Simulation, Modeling and Programming for Autonomous Robots*. pp 147-156

[30] Haeufle, D.F.B., Gunther, M., Bayer, A., and Schmitt, S., 2014, “Hill-Type Muscle Model With Serial Dampening and Eccentric Force-Velocity Relation,” *Journal of Biomechanics*, **47** pp. 1531-1536

[31] Winters, J.M., Woo, S.L.-Y. 1990, *Multiple Muscle Systems: Biomechanics and Movement Organization*. New York: Springer-Verlag. Pp. 69-93, Chap. 5

[32] Graham, D., and McRuer, D.T., 1971, "Phase Plane Analysis," in *Analysis of Nonlinear Control Systems*, Dover Press

BIOGRAPHICAL SKETCH

Philip New is a Master's student at Arizona State University working in the Human Machine Integration Laboratory (HMIL) with Dr. Thomas G. Sugar. He received his Bachelor's Degree of Science and Engineering in Engineering from Arizona State University on the Polytechnic Campus. He was awarded the National Physical Science Consortium Fellowship which is given to graduate students who work for government agencies and laboratories as well as select private industry entities. Phil has worked for Sandia National Laboratories since 2012 and will continue his work in Albuquerque, NM upon completion of his degree. In addition to his duties as a full time student and a member of technical staff at SNL, he is a husband to Danelle and father to Cameron New. It is these duties that he is most looking forward to participating in when the hard work of earning the academic accolades has been completed.